DOE/FE/40812-1

SYNTHESIS OF SULFUR-BASED WATER TREATMENT AGENT FROM SULFUR DIOXIDE WASTE STREAMS

Final Technical Progress Report

Reporting Period Start Date: September 1, 2000
Reporting Period End Date: August 31, 2004

Principal Author(s):
Robert C. Brown, Maohong Fan and Adrienne Cooper

Date Report Issued:
November, 2004

DOE Award Number:
DE-FG26-00NT40812

Submitted By:
Center for Sustainable Environmental Technologies
Iowa State University
285 Metals Development Bldg.
Ames, IA 50011-3020

DISCLAIMER

This report was prepared as an account of work sponsored by an agency of the United States Government. Neither the United States Government nor any agency thereof, nor any of their employees, makes any warranty, express of implied, or assumes any legal liability or responsibility for the accuracy, completeness, or usefulness of any information, apparatus, product, or process disclosed, or represents that its use would not infringe privately owned rights. Reference herein to any specific commercial product, process, or service by trade name, trademark, manufacturer, or otherwise does not necessarily constitute or imply its endorsement, recommendation, or favoring by the United States Government or any agency thereof. The views and opinions of authors expressed herein do not necessarily state or reflect those of the United States Government or any agency thereof.

ABSTRACT

Absorption of sulfur dioxide from a simulated flue gas was investigated for the production of polymeric ferric sulfate (PFS), a highly effective coagulant useful in treatment of drinking water and wastewater. The reaction for PFS synthesis took place near atmospheric pressure and at temperatures of 30-80°C. SO_2 removal efficiencies greater than 90% were achieved, with ferrous iron concentrations in the product less than 0.1%. A factorial analysis of the effect of temperature, oxidant dosage, SO_2 concentration, and gas flow rate on SO_2 removal efficiency was carried out, and statistical analyses are conducted. The solid PFS was also characterized with different methods. Characterization results have shown that PFS possesses both crystalline and non-crystalline structure. The kinetics of reactions among $FeSO_4 \cdot 7H_2O$, $NaHSO_3$ and $NaClO_3$ was investigated.

Characterizations of dry PFS synthesized from SO_2 show the PFS possesses amorphous structure, which is desired for it to be a good coagulant in water and wastewater treatment.

A series of lab-scale experiments were conducted to evaluate the performance of PFS synthesized from waste sulfur dioxide, ferrous sulfate and sodium chlorate. The performance assessments were based on the comparison of PFS and other conventional and new coagulants for the removal of turbidity and arsenic under different laboratory coagulant conditions.

Pilot plant studies were conducted at Des Moines Water Works in Iowa and at the City of Savannah Industrial and Domestic (I&D) Water Treatment Plant in Port Wentworth, Georgia. PFS performances were compared with those of conventional coagulants. The tests in both water treatment plants have shown that PFS is, in general, comparable or better than other coagulants in removal of turbidity and organic substances.

The corrosion behavior of polymeric ferric sulfate (PFS) prepared from SO_2 and ferric chloride (FC) were compared. Results showed that both temperature and concentration of the coagulants substantially impact corrosion rates. The corrosion rates increased with the increase of temperature and concentration. The results from a scanning electron microscope (SEM) showed that chloride caused more serious pitting than sulfate anion on both aluminum and steel specimens. Although SEM confirmed the existence of pitting corrosion, the results of weight loss indicated that the uniform corrosion predominate the corrosion mechanism, and pitting corrosion played a less important role. The test proved that PFS was less corrosive than FC, which may lead to the large-scale application of PFS in waste treatment.

The kinetics of the new desulfurization process has been studied. The study results provide the theoretical guidance for improving sulfur removal efficiency and controlling the quality of PFS.

TABLE OF CONTENTS

Disclaimer i

Abstract ii

Table of Contents iv

Introduction 5

Executive Summary 7

Experimental 9

Results and Discussion 37

Conclusions 88

References 90

Appendices 93

INTRODUCTION

The U.S. Department of Energy's Vision 21 calls for new fossil fuel power generation facilities to be coal refineries, where industrial ecology is an important consideration in their design. Industrial ecology describes a system for achieving sustainability in human industrial endeavors, borrowing principles from natural ecosystems to optimize flows of materials and energy between processes, industries, and communities. It is a compelling design philosophy because it reduces the adverse environmental impacts of industrial production processes.

In these facilities coal will be gasified and the gas stream cleaned of sulfur and other pollutants prior to combustion or conversion to chemical products. Conventional desulfurization processes involve lime chemistry where byproducts are either of relatively low value, such as gypsum, or they are waste products requiring storage and eventual landfilling. However, new technologies involving regenerable sulfur sorbents have been devised, and many are proven effective for Integrated Gasification Combined Cycle applications. These processes remove more than 90% of the sulfur from the hot fuel gas and release it as sulfur dioxide during sorbent regeneration.

The research discussed in this paper investigates use of this sulfur dioxide as a feedstock for synthesis of polymeric ferric sulfate (PFS), a highly effective coagulant used in drinking water and wastewater treatment. PFS is described chemically as $[Fe_2(OH)_n(SO_4)_{(6-n)/2}]_m$ where m is a function of n, $n<2$. The polymeric (pre-hydrolyzed) nature of PFS offers higher Fe to SO_4 ratios than ferric sulfate, and consumes less alkalinity during its use due to the hydroxyl groups included in the polymer structure. There is also evidence in the literature that PFS yields a lower rate of floc size

development, suggesting a lower rate of formation of hydroxide precipitates and therefore a faster interaction with contaminates, in comparison with ferric sulfate. It is effective at removing turbidity, as well as some heavy metal contaminates such as arsenic, at lower temperatures and dosages than other agents. It has also been found in this study to be at least as effective as ferric chloride in removal of disinfection byproduct precursors. PFS has been used in place of alum-based agents in some countries because of concerns with lifetime cumulative aluminum intake playing a role in the development of neurological disorders such as Alzheimer's disease. Meanwhile, preliminary toxicity studies indicate that drinking water treated with PFS is safe for consumption .

Benefits of the process are several. Synthesis proceeds at benign reaction conditions relative to other processes described in the literature [15], thereby reducing construction costs. In addition, it releases no hazardous byproducts into the environment, ensuring that recurring costs associated with material handling and disposal will be lower as well. Overall, we propose an economically and environmentally beneficial solution for sulfur dioxide control.

Executive Summary

The major focus of this research was to investigate the absorption of sulfur dioxide from a simulated flue gas for the production of polymeric ferric sulfate (PFS), a highly effective coagulant useful in treatment of drinking water and wastewater. At temperatures of 30-80°C, SO_2 removal efficiencies greater than 90% were achieved with ferrous iron concentrations in the product less than 0.1%. A factorial analysis of the effect of temperature, oxidant dosage, SO_2 concentration, and gas flow rate on SO_2 removal efficiency was carried out, and statistical analyses are conducted. The product solution was evaluated by wet chemistry methods to verify that the process was capable of consistently producing high quality PFS. Quality parameters examined were total iron concentration, ferrous iron concentration, basicity, density, and pH. It was found that the basicity of PFS could be adjusted by varying how long the absorption and oxidation of SO_2 was continued after all the Fe(II) was converted to Fe(III).

The dried, powdered samples of PFS were analyzed by x-ray diffraction to determine whether drying temperature had an effect on relative crystallinities. All samples examined were highly amorphous, suggesting drying conditions had little influence on crystallinity.

The PFS prepared from SO_2 was evaluated in laboratory. A comparison of the coagulation performance of PFS and ferric sulfate (FS) showed that PFS is, in general, more effective than FS in reducing the turbidity of Kaolinite suspensions for various conditions. The removal of arsenic (V) from water with PFS was investigated under various coagulation conditions and compared with a variety of coagulation agents, including polymeric ferric chloride, polymeric aluminum chloride (PAC), polymeric aluminum sulfate (PAS), ferric chloride (FC), ferric sulfate (FS), aluminum chloride (AC), and aluminum sulfate (AS). Coagulation conditions evaluated include pH, temperature, type of coagulant, the addition of a coagulation aid, and initial As(V) concentration. Results indicated that the arsenic removal efficiencies of polymeric coagulants were generally 10~20% higher than those of their conventional coagulant counterparts. PFS is the best agent to remove As.

To further evaluate the performance of PFS in water treatment, pilot-scale tests were done in Des Moines Water Works and Savannah Industrial and Domestic (I&D) Water Treatment Plant in Port Wentworth, Georgia. Pilot investigation comparing PFS and FC as well as other coagulants showed that in comparison to FC at the same dosages, PFS consumes slightly less alkalinity during treatment, and is, overall, more effective at removing organic matter.

The corrosion behavior of two coagulants, ferric chloride (FC) and PFS, were investigated. Corrosion tests were performed to compare the corrosiveness of these two coagulants on aluminum 6061 and steel 4140 specimens. Results showed that both temperature and concentration of the coagulants substantially impact corrosion rates. The corrosion rates increased with the increase of temperature and concentration. The results from a scanning electron microscope (SEM) showed that chloride caused more serious

pitting than sulfate anion on both aluminum and steel specimens. Although SEM confirmed the existence of pitting corrosion, the results of weight loss indicated that the uniform corrosion predominate the corrosion mechanism, and pitting corrosion played a less important role. The test proved that PFS was less corrosive than FC, which may lead to the large-scale application of PFS in waste treatment.

The kinetics of reactions among $FeSO_4 \cdot 7H_2O$, $NaHSO_3$ and $NaClO_3$ was investigated. The key for the establishment of a kinetic model of the reaction is to find a way to determine concentrations of reactants or products during the reaction. The generation rate of Cl^- during the reaction was monitored using a Dionex Series 4000i ion chromatograph. Based on the changes of Cl^- concentrations at the designed initial reaction conditions, reaction orders for each reactant were derived. The reaction orders were determined to be 1.1 for $NaClO_3$, 1.1 for $FeSO_4$ and 1.4 for $NaHSO_3$. The kinetics model of desulfurization reaction can be expressed as follows:

$$\frac{dc_{Cl^-}}{dt} = k(c_{NaClO_3,0} - c_{Cl^-})^{1.1}(c_{FeSO_4,0} - 2c_{Cl^-})^{1.1}(c_{NaHSO_3,0} - 2c_{Cl^-})^{1.4}$$

where k represents the global rate coefficient and exponents. Furthermore, the pre-exponential factor and the activation energy in the empirical Arrhenius form of the reaction were derived from the relationship between temperature and its corresponding observed global rate coefficient. The global rate coefficients of the reaction at temperatures ranging from 40 to 80 ºC were determined. The Arrhenius form of the desulfurization reaction can be expressed as

$$k = 7.2 \times 10^{12} \cdot e^{-\frac{8291}{T}} (mol^{-2.6} \cdot dm^{2.6} \cdot s^{-1}).$$

EXPERIMENTAL

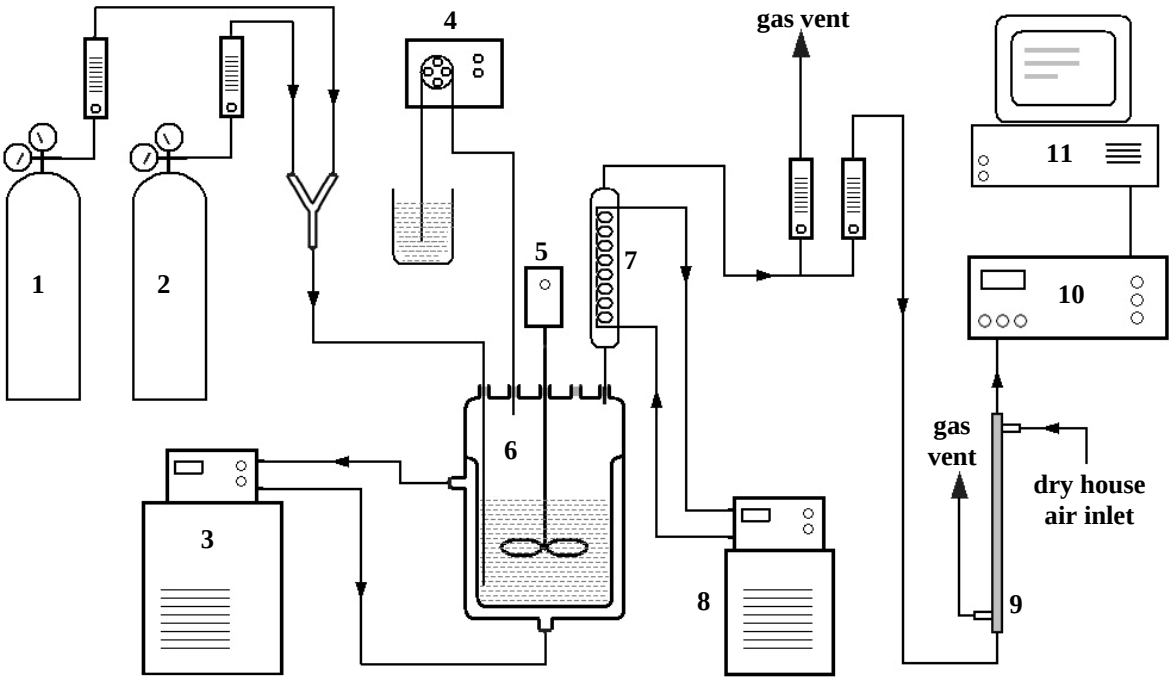
Part I. Synthesis of polymeric ferric sulfate from SO_2

A factorial test was designed to examine the effects of the following four factors on Fe(II) oxidation rate and SO_2 removal efficiency: temperature, SO_2 concentration, nitrogen flowrate, and oxidizer dosing rate. Two levels of each of these four variables were chosen, based on what conditions could be produced reliably in the laboratory. Statistical analyses were performed on the SO_2 removal efficiency data and are presented in the discussion section. In addition, the effect of temperature alone was examined by conducting a set of trials with all variables held constant while temperature was varied between approximately 35 and 80°C.

Equipment

The synthesis system consisted in general of a simple simulated sulfur gas being sparged into a temperature-controlled reactor containing a solution of ferrous sulfate and water, from which the outlet gas was collected and analyzed. In addition, periodic liquid samples were analyzed. A schematic diagram of the system is shown in Figure 1.

The reaction vessel used was a 4 dm^3 jacketed, sealed glass reaction vessel (Chemglass, Inc., Vineland, NJ). A low-temperature silicone oil (Ace Glass, Inc., Vineland, NJ) was circulated through the jacket by a heated and refrigerated Neslab RTE-111 temperature bath unit. The reactor's outlet gas stream passed through a condenser, which was maintained at approximately 3°C by a Cetac Model 2050 chiller. From there, the sample stream passed through a Permapure model MD-110-48 Nafion tube dryer



1. nitrogen tank
2. sulfur dioxide tank
3. temperature controller
4. oxidizer pump
5. stirrer motor
6. jacketed reaction vessel
7. condenser
8. condenser chiller unit
9. sample gas dryer
10. sulfur dioxide analyzer
11. data acquisition computer

Figure 1. Schematic of PFS synthesis system.

(Permapure, Inc., Toms River, NJ) and then through a Cole-Parmer 0.2 micron in-line particulate filter. Finally, the sample stream entered a California Analytical Inc. model ZRF NDIR analyzer (manufactured by Fuji Electric Company, Saddle Brook, NJ) and then was discharged into the lab fume hood. The gas analyzer reads zero to 10% SO_2 to 0.01%, and has repeatability of ± 0.5% of full scale. It also generates a low-voltage DC signal that was recorded by a desktop computer via a data acquisition board.

The reaction mixture was stirred at 200 ± 20 rpm for all trials by an adjustable overhead stirrer connected to a Teflon-coated steel shaft and a Teflon impeller. A Cole-

Parmer Masterflex model 7553-50 peristaltic pump added sodium chlorate oxidizer solution through a neoprene drip tube in the top of the reactor at a rate controlled by a ChronTrol model XT digital timer (ChronTrol, San Diego, CA). Mass measurements of the ferrous sulfate, water, and oxidant solution were measured to 0.1 g on a Mettler model PM4000 balance. The gas was sparged into the reactor via an 8 mm glass tube, and reaction temperature was measured with a non-mercury glass thermometer inserted into the reaction mixture. Periodic liquid samples were drawn with an additional 8 mm glass tube temporarily inserted through the top of the reactor. All surfaces in contact with the reaction mixture were either Teflon or glass.

Reagents

The ferrous sulfate used in the tests was QC Diamond Brand agricultural ferrous sulfate monohydrate (QC Corporation, Cape Girardeau, MO). The sodium chlorate used was Fisher ACS Certified sodium chlorate. The sulfur dioxide was Sulfur Dioxide, Anhydrous, 99.98% from Matheson Tri-gas Inc., Montgomeryville, PA. All other reagents used were Fisher ACS Certified unless otherwise specified.

The ferrous sulfate was analyzed in the lab for Fe(II) content, and it was found to be 96.5 ± 1.4% pure relative to stoichiometrically pure ferrous sulfate monohydrate. This number was used in the subsequent batch calculations. The oxidant as used in the reaction was a liquid solution of 33.3 mass-% sodium chlorate in distilled water.

Design of Factorial Synthesis Runs

The calibration of the gas analyzer was verified daily using 1.00% SO_2 in nitrogen (BOC Gasses, Des Moines, Iowa). The zero point was set using dried, filtered house air. Prior to each run, 630.0 g of ferrous sulfate and 874.5 ± 0.5 g water were weighed out and added to the reactor. Similarly, the mass of oxidant solution was also taken before and after the reaction, allowing the amount consumed to be determined.

After adding the ferrous sulfate and water to the empty reactor, the mixture was stirred for approximately 30 minutes before the reaction began to allow the solids to dissolve and the mixture to equilibrate to the temperature of the reactor jacket. At that point, the simulated sulfur gas flow was started, consisting of a blend of SO_2 and nitrogen gases. The gas flowrates were controlled by rotameters, with each inlet concentration being verified by the gas analyzer for use in subsequent removal efficiency calculations. The interval dosing of oxidizer solution was also started with the gas flow. The dosing of oxidizer was set to be one three-second injection of solution every one, two, or three minutes, with each injection containing approximately 0.6 g of sodium chlorate. Details of the reaction conditions are given in Table 1.

Samples were taken from the reactor periodically and analyzed immediately for Fe(II) content. Samples were pulled by opening a port in the reactor lid, inserting a clean glass tube and drawing in a few milliliters of the reaction mixture. Time and temperature were recorded with each sample.

Table 1. Factorial test conditions and results.

Trt.	Ox. dose (g/min)	Temp. (°C)	SO_2 conc. (%)	N_2 flow (l/min)	SO_2 dose (ml/min)	Fe conv. rate (g/hr)	SO_2 removal (% of inlet)
1	0.60	39.9	1.9	1.2	22.7	126.2	99.5
2	0.59	41.0	2.2	5.0	114.6	107.5	82.6
3	0.60	42.2	5.4	1.2	68.8	114.0	95.6
4	0.59	43.2	5.3	5.0	277.0	89.4	53.2
5	0.61	61.1	1.9	1.2	22.9	135.0	98.0
6	0.60	60.3	2.2	5.0	114.6	119.1	75.8
7	0.69	63.9	5.4	1.2	68.8	117.5	87.8
8	0.60	60.9	5.3	5.0	277.0	100.7	47.4
9	0.20	34.8	1.9	1.2	22.9	35.4	94.3
10	0.21	34.2	2.2	5.0	114.6	36.5	45.4
11	0.19	35.0	5.4	1.2	68.8	27.8	67.9
12	0.20	34.4	5.3	5.0	277.0	25.2	16.9
13	0.19	57.6	1.9	1.2	22.9	39.8	79.8
14	0.19	54.7	2.2	5.0	114.6	33.5	34.9
15	0.20	57.9	5.4	1.2	68.8	33.4	49.2
16	0.20	54.5	5.3	5.0	277.0	28.7	15.5
mid	0.30	47.6	3.7	3.1	117.3	51.2	46.9
mid	0.32	47.9	3.7	3.1	117.3	50.6	50.8
mid	0.31	47.0	3.7	3.1	117.3	49.9	50.0
mid	0.31	47.8	3.7	3.1	117.3	52.3	50.2
mid	0.31	47.6	3.7	3.1	117.3	48.2	51.3
r3	0.61	39.0	5.4	1.2	68.0	123.8	93.0
r8	0.62	59.0	5.3	5.0	277.0	107.1	47.5
r12	0.20	34.2	5.3	5.0	277.0	28.2	24.2
r16	0.22	56.4	5.3	5.0	277.0	31.7	18.0

Analysis of liquid PFS product

Quality parameters for the liquid PFS are well established in the literature [1-2]. The analyses used were total iron, ferrous iron, and basicity (sometimes referred to as B-value). Density and pH were also measured.

The total iron content of the PFS was measured by taking a 1.5 g sample of the liquid PFS product and acidifying it with hydrochloric acid. The sample was then heated to boiling, and all iron was reduced to Fe^{2+} by addition of stannous chloride and titanium trichloride. A titration was then performed using a standardized potassium dichromate

titrant, with diphenylamine sodium sulfonate indicator. The titration reaction is given here in Equation (1), and the subsequent calculation of total iron in Equation (2).

$$6Fe^{2+} + Cr_2O_7^{2-} + 14H^+ \rightarrow 6Fe^{3+} + 2Cr^{3-} + 7H_2O \qquad (1)$$

$$X_1 = \frac{(V)(C)(0.05585)(6)}{M} \times 100\% \qquad (2)$$

X_1=total iron concentration (mass-%) in the PFS liquid, V=volume (mL) of potassium dichromate titrant consumed, C=molar concentration of the titrant, M=mass (g) of liquid PFS sample, and 0.05585 is the mass in grams of 0.001 mole of iron.

The concentration of ferrous iron was determined with a similar titration. A sample of approximately 2.0 g of liquid PFS product was acidified with sulfuric and phosphoric acids, and then titrated with a standardized potassium permanganate solution. The net reaction occurring in this analysis is shown in Equation (3), and the calculation is given in Equation (4).

$$5Fe^{2+} + MnO_4^- + 8H^+ \rightarrow 5Fe^{3+} + Mn^{2+} + 4H_2O \qquad (3)$$

$$X_2 = \frac{(V - V_0)(C)(0.05585)(5)}{M} \times 100\% \qquad (4)$$

X_2=ferrous iron concentration (mass-%) in the PFS liquid, V=volume (mL) of potassium permanganate titrant consumed, V_0=volume of the titrant consumed by a distilled water blank, C=molar concentration of the titrant, M=mass (g) of liquid PFS sample, and 0.05585 is the mass in grams of 0.001 mole of iron.

The basicity is the mass ratio of OH^- to Fe^{3+} in the polymer, which gives an indication of the degree to which the iron has been hydrolyzed [1-2]. Furthermore, it can be used as a measurement of the extent of polymerization according to the chemical formula for PFS. Basicity was measured by taking a 1.5 g sample of the liquid PFS

product and adding to it a known quantity of dilute hydrochloric acid. After allowing the mixture to stabilize for 10 minutes, a small amount of potassium fluoride was introduced to shield the iron, and phenolphthalein was added as an indicator. The solution was then titrated with dilute sodium hydroxide to find the quantity of acid neutralized by the polymer. The basicity is calculated as shown in Equation (5).

$$B = \frac{\frac{(V - V_0)(C)(0.0170)}{17.0}}{\frac{(M)(X_1 - X_2)}{18.62}} \times 100\% \qquad (5)$$

B=ratio of OH^- to Fe^{3+} (mass-%), V=volume (mL) of sodium hydroxide titrant consumed, V_0=volume of the titrant consumed by a distilled water blank, M=mass (g) of liquid PFS1 sample, C=molar concentration of the titrant, 17.0= mass (g) of one mole of OH^-, 0.017= mass (g) of 0.001 mole of OH^-, and 18.62= mass (g) of 1/3 mole iron.

Density of the liquid PFS product was measured using a 10 mL Gay-Lussac adjusted density bottle (supplied by Cole Parmer). A direct correlation was found between total iron content and density of the liquid PFS product, allowing a measurement of one of these parameters to be used to estimate the other. pH was measured from a 1 mass-% solution of the liquid PFS product in water, using a Corning pH Meter 320 calibrated with Fisher certified buffers at pH 1.00 ± 0.02 and pH 4.00 ± 0.02. All titrant solutions and calibrations were made using Fisher ACS Certified chemicals and deionized water.

Table 2 shows the acceptable range of the PFS quality parameters used in this study. Basicity and pH ranges given are based on acceptable behavior of liquid PFS in storage and treatment. Too high of either value decreases the stability of the product, with an a tendency to form precipitates [1]. Meanwhile, a low basicity value indicates a

lower degree of polymerization. A very low Fe(II) content is desirable since this species has a tendency to stain fixtures and surfaces and is difficult to precipitate.

Table 2. PFS quality parameters and optimal value ranges.

pH (1 mass-% solution)	Total iron (mass-%)	Iron(II) (mass-%)	Density (g/cm^3)	Basicity (mass-%)
2.0-3.0	≥ 9.0	≤ 0.1	≥ 1.3	8.0-12.0

Characterization of solid PFS

Samples of approximately 2.5 g liquid PFS were dried on standard watch glasses in a Fisher Isotemp model 725G gravity oven. Two samples came from a batch of PFS that was approximately one week old, and had an Fe(II) concentration less than 0.1% and a basicity of 10.1%. Both samples were dried for 12 hours, one at 60°C and the other at 90°C. A third sample, which was dried at 80°C for 16 hours, was also included for comparison. It was taken from a batch of PFS approximately five months old, and had an Fe(II) concentration of less than 0.1% and basicity of 7.8%.

After the stated drying period, the samples were removed from the oven and immediately ground vigorously for three minutes in a mortar and pestle. They were then stored in sealed vials until their analysis. The two samples dried for 12 hours were stored for approximately six weeks before analysis, while the third sample was produced earlier and stored for approximately 10 weeks before its analysis.

The x-ray analyses were carried out using a Philips 1830/00 vertical goniometer and generator unit controlled by a Philips 1710 APD controller. The x-rays were generated from a copper source operated at 40 kV and 20 mA. Powder samples were

placed in a hollow glass slide and scanned from 20° to 120° by 0.2° in the 2 θ configuration.

Lab-scale evaluation of PFS

Removal of Turbidity

Suspensions were prepared for testing the PFS coagulant by dispersing kaolin (Wilkinson Kaolin Assoc. Ltd., Gordon, GA) in water mixtures composed of 30% Ames city tap water with a turbidity of 0.3 NTU and 70% distilled water. The dissolved organic carbon (DOC) of Ames city tap water is less than 0.02 ppm. The purpose to mix Ames tap water with hardness level in the range of 160-180 ppm and distilled water is to lower the hardness level of the tested water to a moderate level of 110-130 ppm. The concentration of Kaolinite in the prepared stock suspension was 10 g/l. Other suspensions for testing were prepared by diluting the stock solution with the aqueous medium to 10 NTU and 100 NTU, respectively. The alkalinity of the diluted (tested) suspensions was regulated with $NaHCO_3$ to 45 mg/l as $CaCO_3$. Either 0.1 M HCl or 0.1 M NaOH solution was added to the diluted (tested) suspensions to regulate pH, as necessary.

The jar tests were conducted to compare the coagulating behavior of the PFS and FS at different dosages and under various initial pH values of suspensions. The jar tests were performed using a Phipps & Bird model PB-700^{TM} jar tester, which consisted of 2-liter square acrylic plastic jars, each jar fitted with a flat blade paddle. Each jar had a sample tap at a point about 10 cm below the water line to withdraw samples. To begin a jar test, all six jars were first filled with a 2000 ml dilute suspension. Next, a stirring

speed of 80 rpm was set and the suspensions were stirred for 10 minutes to disperse the Kaolinite particles homogeneously and to reach equilibrium with the atmosphere. Then various dosages of prepared coagulant solutions were added to the suspensions. In view of the PFS solution concentration and amount of water in the jars, a stirring speed of 250 rpm was used for 1 minute of rapid mixing, followed by a stirring speed of 30 rpm for 30 minutes of slow mixing. Finally, the suspensions were left to settle for 30 minutes except where the effect of setting time on residual turbidity was investigated. The turbidity of the suspensions before and after coagulation was measured with a Cole Parmer model 8391-40 turbidity meter.

Removal of Arsenic

Except for the coagulants used in As(V) removal experiments, all chemicals were reagent-grade, and were employed without pretreatment. Solutions of 0.51 M stock ferric sulfate, 0.51 M stock ferric chloride, 0.53 M stock aluminum sulfate, and 0.53 M stock aluminum chloride were prepared by dissolving appropriate quantities of the above salts into de-ionized water.

All polymeric iron and polymeric aluminum coagulants were prepared in the laboratories of Center for Sustainable Environmental Technologies, Iowa State University. Polymeric ferric chloride (0.51 M) with a basicity of 11%, polymeric aluminum sulfate (0.53 M) with a basicity of 51%, and polymeric aluminum chloride (0.53 M) with a basicity of 51% were prepared by sodium carbonate (1 M) titration at 25.0°C [3-5].

In order to enhance arsenic removal, activated silica solution was used as a coagulant aid in the coagulation process. The first step in preparing activated silica is to dilute sodium silicate (Na_2O:2.5SiO_2, 49-52° Bé, Fisher Scientific) with de-ionized water to a 5 wt-% solution. Next, sulfuric acid was slowly added to the solution until pH decreased to 6.5, which was monitored with an Orion Research, Inc. model 250A pH meter. The last step was to allow the acidified solution to age for 2 hours before it was used for coagulation tests.

It must be mentioned that As (V) is the prevalent arsenic species in most surface water and it is easier to remove by precipitation than As (III) [6]. The removal of total arsenic can be readily achieved by oxidizing As (III) to As(V). Therefore, we only focus on the removal of As (V).

A stock solution of As (V) in water was prepared from the sodium salt heptahydrate, $Na_2HAsO_4 \cdot 7H_2O$ (Matheson, Coleman & Bell) at a concentration of 1 g/L. Secondary solutions of 100 mg/L arsenic concentration were freshly prepared as needed by diluting stock solution with de-ionized water.

The stock Kaolinite suspensions used in coagulation tests were prepared by dispersing Kaolinite into de-ionized water (Wilkinson). The concentration of Kaolinite in the stock suspension was 8 g/L. Other than those specified, the initial turbidity and arsenic concentrations of the suspensions used for coagulation tests were controlled at close to 15 NTU and 50 μg/L, respectively. The pH levels of tested suspensions were adjusted to initial equilibrium values of 5.5, 7.0, and 8.5 by adding either 1.0 M HNO_3 or 1.0 M NaOH.

Jar tests were conducted to evaluate the arsenic removal efficiency of coagulants under different coagulation conditions, including temperature, initial pH, type and dosage of coagulant, addition of activated silica, and initial arsenic concentration of the prepared suspensions. The tests were performed using a Phipps & Bird model PB-700^{TM} jar tester (General Medical Mfg. Co., Richmond, VA). Each jar has a sample tap at a point about 10 cm below the water line to withdraw samples. The first step in the jar tests was to stir the tested suspensions (2 L) in jars at 100 rpm for 5 minutes, which dispersed the Kaolinite particles homogeneously, thus permitting them to reach equilibrium with the atmosphere. The prepared arsenic solution, coagulant, and activated silica (when required), were then dosed into the suspensions. The solution was flash-mixed at 250 rpm for one minute, followed by slow mixing at 30 rpm for 25 minutes. Finally, the suspensions were left to settle for 25 minutes. After settling, roughly 150 ml of supernatant was removed from the jar through the sampling tap and apportioned into two aliquots. One part was immediately used to measure the turbidities and analyze arsenic concentration. The other portion was filtered through a 0.45 μm cellulose acetate membrane (Fisher), after which the final turbidity and arsenic concentration were also measured.

The concentration of arsenic in the water was measured with a 4500 series ICP-MS (Hewlett-Packard Co., Foster, CA). The instrument was calibrated with a set of arsenic standards at concentrations of 0, 10, 15, 30, 40 and 50 ppb. The 50 ppb standard was also run before and after a set of samples.

Pilot-scale evaluation of PFS

Tests in Des Moines Water Works

Pilot tests of the liquid PFS were conducted at the Des Moines Water Works (DMWW) facility in Des Moines, Iowa. PFS and ferric chloride, the agent currently used there, were compared for their ability to remove several typical dissolved and colloidal pollutants. The pilot system was designed previously by the DMWW laboratory staff as an operating model of their production facilities, and therefore a good deal was known about the operation of the system before starting the PFS study.

For these trials the flow rate through the pilot system was approximately 2 L/min, with a residence time on the order of six hours. A schematic diagram is shown in Figure 2. The first stage is a presedimentation block in which an initial dose of coagulant is added to raw river water, which makes up approximately half of the total output of the plant. After flocculation and settling sections, the flow continues into the treatment stage

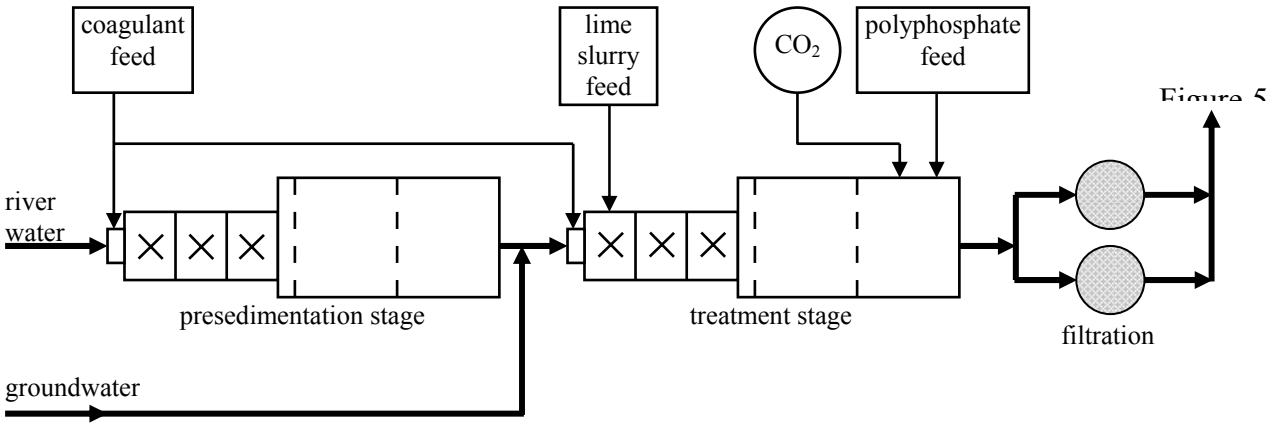


Figure 2. Flow chart of Des Moines Water Works pilot-scale plant.

where it is augmented by approximately the same volume of water taken from a series of shallow wells a short distance inland from the riverbank. This water is much less turbid, and therefore doesn't require the pre-sedimentation step. At the inlet of the treatment stage an additional dose of coagulant, equal to twice the first, is added to the flow. Lime slurry is also dosed to achieve a pH of 10.6 in the flocculation zone following the last mixer. Just before leaving the treatment stage, a small amount of CO_2 is added to the water to reduce the pH to the final production level. A small dose of polyphosphate is also added to prevent lime caking in the filters. Final filtration is effected with two parallel sand filtration columns.

Premixed stock solutions of PFS and ferric chloride (FC) were prepared at 2 mg/L, 3 mg/L, and 4 mg/L (as Fe), with approximately 3 g/L sulfuric acid added to the PFS solutions and a similar quantity of hydrochloric acid added to the FC solutions to reduce precipitation. The PFS used for the pilot trials was approximately five months old, and had a total Fe concentration of 9.7 wt-% and a basicity of 7.8 wt-%. The residual Fe(II) concentration was negligible. Each agent-dose combination was started in the afternoon, and the system was allowed to stabilize overnight. The next day, six hourly turbidity samples were taken before the next agent-dose combination was started. The two coagulant types were dosed through the system on alternating days. Measurements of turbidity were made at three points: raw water, end of pre-sedimentation stage, and end of treatment stage (pre-filter), using a Hach 2100AN turbidimeter calibrated daily with Gelex Secondary Standards. The following measurements were also made of the raw and pre-filtered waters at the time of the last turbidity sample (with the exception of those at the 4 mg/L dose, which were taken with

the first turbidity sample): total organic carbon (TOC) and dissolved organic carbon (DOC) by a Shimadzu TOC-5000, ultraviolet light absorbance at a wavelength of 254 nm (UV-254) by a Shimadzu 1201 UV-VIS, and total alkalinity by titration. Analyses were made in the DMWW laboratory.

Tests in City of Savannah Industrial and Domestic (I&D) Water Treatment Plant

The PFS synthesized from SO_2 for pilot-scale tests in City of Savannah Industrial and Domestic (I&D) Water Treatment Plant contains 11.5 wt-% Fe, and its basicity (B value, mass of OH^-/ mass of total Fe) is of 8.5 wt-%. The ferric sulfate and ferric chloride were purchased from Kemiron. The ferric chloride used contains 13.8wt-% iron (III) while the ferric sulfate used contains 12.78 wt-% iron (III). Both solutions met or exceeded American Water Works Association (AWWA) standards and were ANSI/NSF Standard 60 certified. The alum used in the study was provided by General Chemical and contained 7.66 wt-% aluminum.

The raw water used in the study was surface water obtained from a tributary of the Savannah River. The water was not pretreated in any manner before initial feed to the pilot plant. Because of the tidal effects experienced in the tributary, typical water quality determinants are not available; however, ranges of the raw water parameters can be found in Table 3**.**

Samples were collected from the pilot plant at either 6-hour or 12-hour intervals. The frequency depended on the length of the experimental run, which was a function of

Table 3. Typical Raw Water Quality

Determinants	Range
TOC, mg/l	5 - 8
TSS*, mg/l	1 - 10
TDS**, mg/l	55 - 85
Nitrate, mg/l	0 - 1
Sulfate, mg/l	0 - 15
Iron, mg/l	1 - 2
Aluminum Residual, mg/l	0.03 - 0.05
True Color	55 - 110
Total Hardness, mg/l $CaCO_3$	24 - 30
Specific Conductance	85 - 125
Alkalinity, mg/l $CaCO_3$	19 - 30
CO_2, mg/l	9 - 20
Chloride, mg/l	8 - 15
Turbidity, NTU	12 - 16

* TSS: Total suspended solids
** TDS: Total dissolved solids

the volume of coagulant available for testing. Analytical samples were collected in sterile one-liter bottles. Samples for TOC analysis were collected separately and stored in dark bottles containing sulfuric acid for preservation until analysis.

All of the water samples in the pilot plant were analyzed for iron, aluminum, sulfate, nitrate, total organic carbon, alkalinity, suspended solids (TSS), dissolved solids (TDS), true color, hardness, specific conductance, and chlorides (where appropriate). The analyses were conducted by the lab personnel at the City of Savannah Industrial and Domestic (I&D) Water Treatment Plant using EPA approved methods [11].

Before initial startup of the pilot plant, jar tests were conducted to determine the dosage required to adequately treat the water as it passes through the pilot plant. Due to frequent changes in the water quality, jar tests were also conducted periodically during

the experiment. This was required to maintain the proper dosage for adequate treatment and mirrors the process followed for the associated operating plant. The study involved comparison of the iron-based coagulant to the traditional coagulant, aluminum sulfate, in an effort to determine differences in final water quality.

Jar tests were conducted using a six paddle jar-test apparatus (Phipps & Bird, Model 7790-400) at room temperature (~20 °C). The six beakers were filled with 1 L samples of the raw water and the appropriate volume of coagulant was added using a pipette. After coagulant addition the samples were rapid mixed at approximately 200 rpm for one minute followed by a three stage slow mix consisting of five minute intervals at speeds of 60, 40, and 20 rpm, respectively. Slow mixing was followed by a 20 minute settling period. After settling, the supernatant was withdrawn from a depth approximately two inches below the surface. Turbidity was measured on a HACH Model 2100A turbidimeter and pH values were measured using a pocket calorimeter.

To determine the proper dosage a two-step method was performed. The initial step involved testing a wide range of doses typically ranging from 20 mg/L to 70 mg/L. The dosage used in the second step was a spread of 6-9 mg/L above and below the best jar dosage obtained in the first step.

Pilot plant studies were conducted at in a pilot facility owned and operated by the City of Savannah Industrial and Domestic Water Treatment Plant. The pilot plant consists of two identical treatment trains that include a rapid mix basin (76 L), settling basin (15,141 L) and filter (1135 L). Figure 3 is a schematic of a single treatment train of the pilot plant used for the study. The rapid mix basins and the settling basins were designed with serpentine flow to minimize short-circuiting.

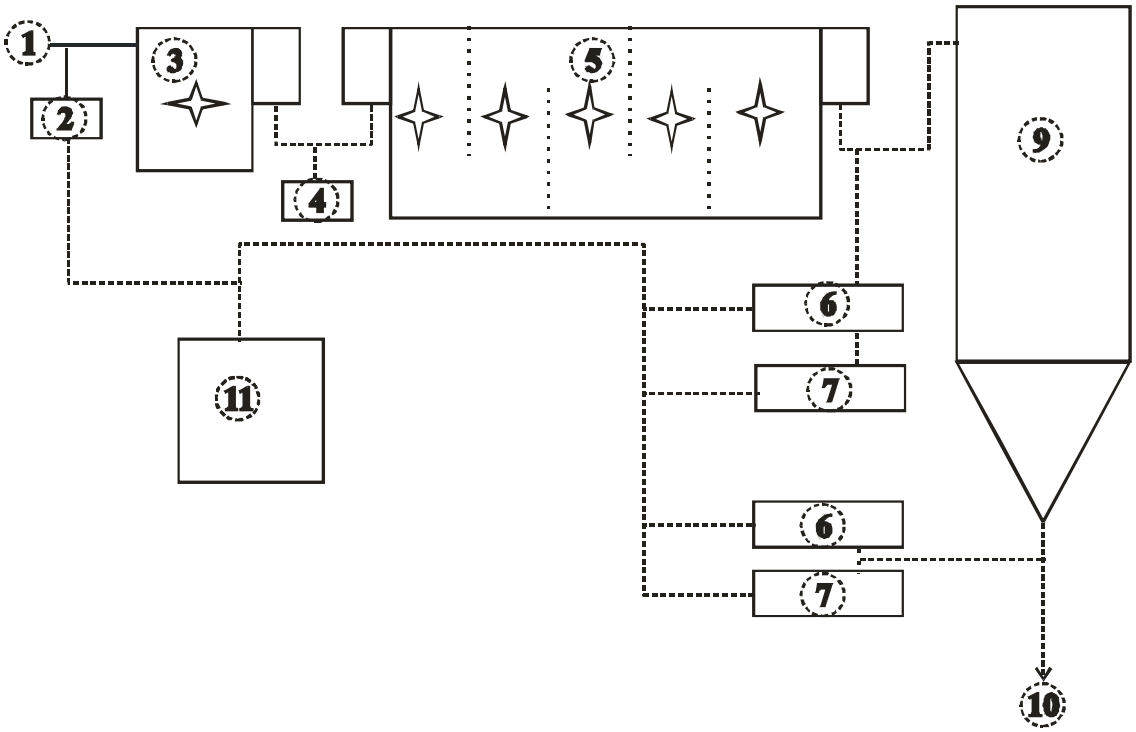


Figure 3. Schematic of Industrial and Domestic (I&D) Water Treatment Pilot Plant.
(1) Raw water, (2) MAG meter, (3) Rapid mix, (4) pH meter, (5) Settling basin, (6) Turbidity meter, (7) Particle counter, (8) Settling basin, (9) Filter (10) Finished water, (11) CPU.

Each individual treatment train is rated for a maximum influent flow of 68 liters per min with a retention time of approximately four hours through the settling basin at maximum flow. The pilot plant filters are anthracite (0.25 meters), sand (0.45 meters), and gravel (0.30 meters). The filters are rated for a flow of 234.7 m^3/m^2d (4 gpm/ft^2).

The pilot plant is equipped with online instrumentation that provides real time measurements. Each treatment train is equipped with a pH electrode, two particle counters and two laser light turbidimeters. The pH electrode is positioned to analyze the pH after rapid mixing has occurred. The particle counters and light turbidimeters are

positioned to analyze the particle counts and turbidity of the settled water and the finished filter water. The raw water line entering the pilot plant is also equipped with a pH electrode and a laser light turbidimeter to determine the raw water quality. The flows into the rapid mix basins and through the filter are measured by online magnetic (MAG) meters.

Evaluation of corrosion

Experiments were designed to compare the degree of corrosion caused by ferric chloride (FC) and PFS. The parameters selected were temperature, concentration of coagulant, and types of specimen material. The test was designed according to the relative standards of American Society for Testing and Materials (ASTM). The standards involved were G1-90 (Reapproved 1999) Practice for preparing, cleaning, and evaluating corrosion test specimens; G3-89 (Reapproved 1999) Practice for conventions applicable to electrochemical measurements in corrosion testing; G16-95 (Reapproved 1999) Guide for applying statistics to analysis of corrosion data; G31-72 (Reapproved 1999) Practice for laboratory immersion corrosion testing of metals.

Reagent grade $FeCl_3.6H_2O$ (Assay 97.3%, Fisher) was dissolved in deionized water to make the FC solution. Two different concentrations of solution were prepared, one containing 1 wt % and the other, 10 wt % Fe(III),

The PFS solutions used for corrosion tests were made in the laboratory of the Center for Sustainable Environmental Technologies (CSET) at Iowa State University (ISU), Ames, USA. Typically, they contained more than 10.5 wt% iron and their

basicities are higher than 11.0%. The synthesized PFS was diluted to 1 wt% Fe(III) and 10 wt% Fe(III) for the corrosion tests.

Two kinds of solutions, phosphoric acid and hydrochloric acid, were made up to treat the corroded specimens and remove the corrosion product. The phosphoric acid solution was made up by mixing 50 mL phosphoric acid (Fisher Scientific, H_3PO_4, specific gravity = 1.69) and 20 g chromium trioxide (Fisher, 99.9%) followed by addition of deionized water to make 1000 mL solution. The hydrochloric acid solution was made up of 1000 mL hydrochloric acid (Fisher Scientific, HCl, specific gravity = 1.19), 20 g antimony trioxide (Sb_2O_3, Aldrich), and 50 g stannous chloride ($SnCl_2$).

Two materials, aluminum 6061 and steel 4140, were used in the corrosion test. The metals were processed at ISU's Chemistry Machine Shop into circular specimens with a diameter of 38 mm and thickness of 3 mm. An 8-mm diameter hole was drilled in the middle for convenient mounting. The average weight of the aluminum and steel specimens were 9.5 g and 27.7 g respectively.

The sample disks were immersed in FC and PFS solutions that both contained 1 and 10 wt% Fe(III) at five different temperature settings, i.e. 5 °C, 20 °C, 35 °C, 50 °C and 65 °C for 10 hours.

To compare the corrosion effects of PFS and FC, the specimens were examined with a Hitachi S-2460N Scanning Electron Microscope (SEM) set at high vacuum mode with 20 kV beam. Micrographs from the SEM were used to investigate the surface morphology of the corroded specimens.

Before testing, the specimens were polished with No. 100 abrasive paper (aluminum oxide, made in Poland) to remove the surface oxidation layer of metal and

eliminate variations on the metallic surface. Final surface treatment was accomplished with No. 180 abrasive paper (silicon carbide, made in Poland) and acetone (Fisher Scientific, 99.0%, density = 0.7847 g/mL). All specimens were weighed with Mettler AE100 Analytical Balance and these initial weights were recorded.

The corrosion test started with the addition of 1000 mL PFS or FC solution into the 1000 mL reactor (ChemGlass). The setup of the experimental apparatus is illustrated in Figure 4. Controlled with a temperature bath unit, the temperature of the reaction solution was stabilized at the set point. After the temperature of solution reached the set point, five specimens were immersed into the solution and timing was started. The

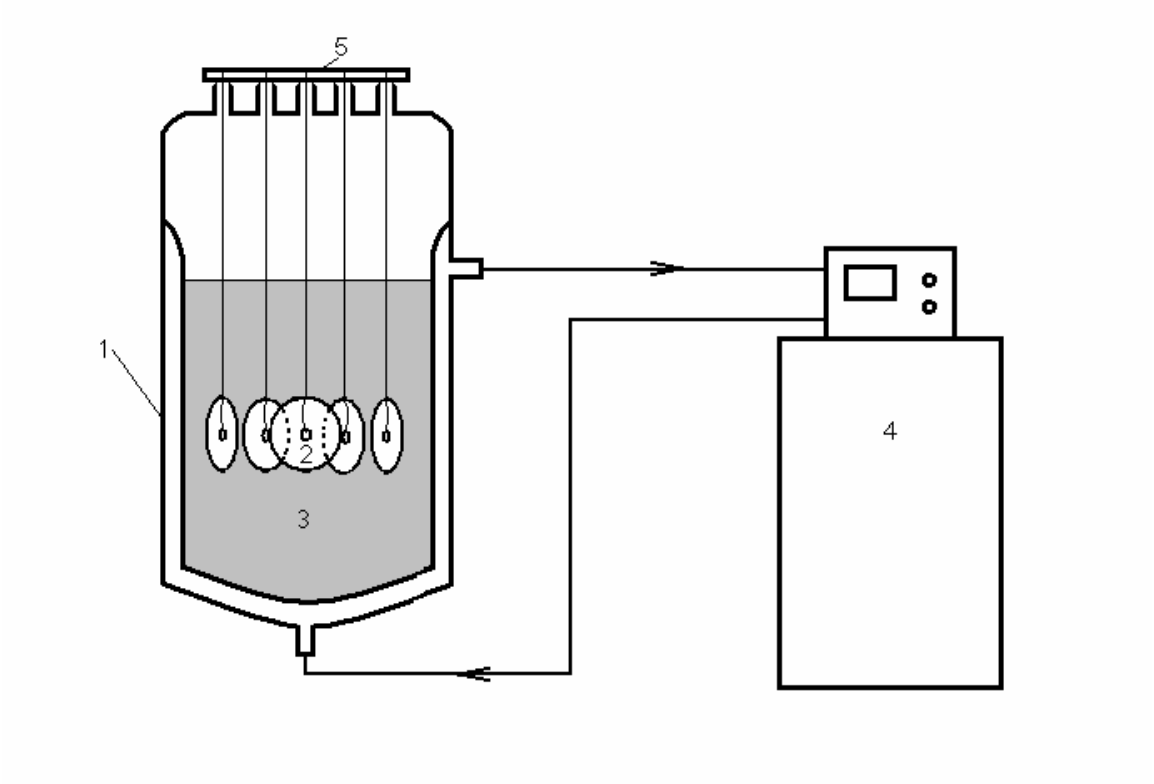


Figure 4. Experimental setup of the corrosion test
(1) Reaction vessel, (2) Corrosion specimens, (3) Coagulant solution, (4) Reactor temperature bath unit, (5) Specimen mounting rack.

specimens were tied to the mounting rack with nylon string and suspended in the solutions to avoid contact with each other.

Every two hours, one specimen was taken out of the reactor, treated with a chemical solution to remove corrosion products, and weight losses were measured. The aluminum specimens were treated with a phosphoric acid solution for 10 minutes at 95 °C followed by washing with water and acetone. The steel specimens were treated with a hydrochloric acid solution for 25 minutes at 25 °C followed by washing with water and acetone. In all cases, the dried specimens were weighed on a balance. The weight of the corroded specimen was subtracted from its initial weight, thus giving the weight after two hours of corrosion. By using the same way, weight losses of specimens at the immersion time of four, six, eight and ten hours were obtained. After the corrosion test, the corroded specimens were examined with SEM surface morphology to determine the effects of types and concentrations of the coagulant solutions on them. Three different magnitudes-50, 200 and 500-were used to acquire the surface morphology.

Study of Desulfurization Kinetics

Theory

SO_3^{2-} and HSO_3^- may simultaneously exist due to the presence of SO_2 in the reaction system. However, the oxidation of Fe^{2+} requires the presence of H^+. Since SO_3^{2-} is unrelated to the oxidation of Fe^{2+}, only HSO_3^- can meet this requirement. Consequently, only the reaction between $NaClO_3$, $FeSO_4$ and $NaHSO_3$ needs to be considered for the production of PFS when the pH of the reaction system is less than 7, which can be realized by continuously bubbling SO_2 into the reactor.

The reaction between $NaClO_3$, $FeSO_4$ and $NaHSO_3$ (prepared from SO_2)can be expressed as follows

$$NaClO_3 + 2FeSO_4 + 2NaHSO_3 \rightarrow NaCl + Na_2SO_4 + Fe_2(SO_4)_3 + H_2O \quad (6)$$

Assuming that $c_{NaClO_3,0}$, $c_{FeSO_4,0}$ and $c_{NaHSO_3,0}$ represent the initial mole concentrations of reactants $NaClO_3$, $FeSO_4$ and $NaHSO_3$, respectively, initial concentration of NaCl is 0, and c_{Cl^-} is the concentration of NaCl or Cl^- generated during the reaction or the quantity of $NaClO_3$ or ClO_3^- consumed, then the concentrations of all the reactants at any time, *t*, should be $c_{NaClO_3,0} - c_{Cl^-}$, $c_{FeSO_4,0} - 2c_{Cl^-}$, $c_{NaHSO_3,0} - 2c_{Cl^-}$, respectively, and the increasing rate of c_{Cl^-} can be expressed as follows

$$\frac{dc_{Cl^-}}{dt} = k(c_{NaClO_3,0} - c_{Cl^-})^{n_1}(c_{FeSO_4,0} - 2c_{Cl^-})^{n_2}(c_{NaHSO_3,0} - 2c_{Cl^-})^{n_3} \quad (7)$$

where *k* represents the global rate coefficient and exponents n_1, n_2, and n_3 are the orders with respect to reactants $NaClO_3$, $FeSO_4$ and $NaHSO_3$. Reaction orders n_1, n_2 and n_3 are not necessarily integers because reaction 6 is not an elementary reaction.

Special initial reactant concentrations need to be designed in order to derive reaction orders n_1, n_2 and n_3. For example, when $c_{NaClO_3,0}$ and $c_{FeSO_4,0}$ are much larger than $c_{NaHSO_3,0}$, c_{NaClO_3} and c_{FeSO_4} at any time t of the reaction 6 can be considered as constants, or

$$c_{NaClO_3} = c_{NaClO_3,0} - c_{Cl^-}$$

$$c_{NaClO_3} \approx c_{NaClO_3,0} \quad (8)$$

$$c_{FeSO_4} = c_{FeSO_4,0} - 2c_{Cl^-}$$

$$c_{FeSO_4} \approx c_{FeSO_4,0}, \quad (9)$$

and then Equation 9 can be simplified as

$$\frac{dc_{Cl^-}}{dt} = k_3(c_{NaHSO_3,0} - 2c_{Cl^-})^{n_3} \quad (10)$$

where $k_3 = kc_{NaClO_3,0}^{n_1} \cdot c_{FeSO_4,0}^{n_2}$. (11)

Taking the logarithm of Equation 11 yields

$$\log\frac{dc_{Cl^-}}{dt} = n_3 \log(c_{NaHSO_3,0} - 2c_{Cl^-}) + \log k_3. \quad (12)$$

The c_{Cl^-} at any time, *t*, of the reaction was measured with a Dionex Series 4000i ion chromatograph, which leads to the establishment of the relationship of c_{Cl^-} vs. time. Consequently, the reaction order with respect to $NaHSO_3$, n_3, can be derived by curve fitting according to Equation 12. It is noted that the value of $\frac{dc_{Cl^-}}{dt}$ at time *t* was obtained from c_{Cl^-} - *t* curve by using a tangential approach [7]. Similarly, when $c_{NaClO_3,0}$ and $c_{NaHSO_3,0}$ are much larger than $c_{FeSO_4,0}$, n_2, can be obtained by curve fitting according to Equation 12, which is based on the relationship of $c_{Cl^-} \sim t$ attained through experimental data. In addition, when the initial concentrations of the reactants $FeSO_4$ and $NaHSO_3$, $c_{FeSO_4,0}$ and $c_{NaHSO_3,0}$, are much larger than $c_{NaClO_3,0}$, the reaction order with respect to $NaClO_3$, n_1, can be inferred by curve fitting the experimental $c_{Cl^-} \sim t$ relationship and its corresponding the plot of Equation 12.

Furthermore, the initial reactant concentrations with the relationship of $2c_{NaClO_3,0} = c_{FeSO_4,0} = c_{NaHSO_3,0}$ were designed to derive global rate coefficient *k* at a known temperature. Given initial concentrations of three reactants, Equation 7 can be reorganized as

$$\frac{dc_{Cl^-}}{dt} = k(c_{NaClO_3,0} - c_{Cl^-})^{n_1} \cdot 2^{n_2}(c_{NaClO_3,0} - c_{Cl^-})^{n_2} \cdot 2^{n_3}(c_{NaClO_3,0} - c_{Cl^-})^{n_3}$$

$$= 2^{n_2+n_3} \cdot k \cdot (c_{NaClO_3,0} - c_{Cl^-})^{n_1+n_2+n_3} \quad (13).$$

Integration of Equation 13 with the boundary condition ($c_{Cl^-,0} = 0$) results in

$$\int_0^{c_{Cl^-}} \frac{dZ}{(c_{NaClO_{3,0}} - Z)^{n_1+n_2+n_3}} = \int_0^t 2^{n_2+n_3}.k dt \quad (14)$$

$$(c_{NaClO_3,0} - c_{Cl^-})^{1-(n_1+n_2+n_3)} - c_{NaClO_3,0}^{1-(n_1+n_2+n_3)} = 2^{n_2+n_3} \cdot k \cdot (n_1+n_2+n_3-1)t \quad (15)$$

or

$$k = \frac{(c_{NaClO_3,0} - c_{Cl^-})^{1-n_1+n_2+n_3} - c_{NaClO_3,0}^{1-(n_1+n_2+n_3)}}{2^{n_2+n_3}(n_1+n_2+n_3-1)t}. \quad (16)$$

Therefore, the global rate coefficient *k* at a specified temperature can be determined using Equation 11 given that n_1, n_2 and n_3 have been obtained, and c_{Cl^-} at time *t* is measured.

The temperature range, 40-80 ˚C, important for the $FeSO_4$-based sulfur removal approach, is reasonably narrow, consequently variations of the pre-exponential factor and the activation energy of reaction 6 with temperature can be ignored [8-9]. Therefore, the relationship between the global rate constant (*k*) and reaction temperature (T) can be expressed in the empirical Arrhenius form below

$$k = A\exp(-\frac{E}{RT}) \quad (17)$$

where A is the pre-exponential factor, E is the activation energy of reaction 6 and R is the ideal gas constant. The plot of log *k* versus 1/T can be used to extract values for A and E in Arrhenius form (Equation 17), since the slope and interception of such a plot are -E/2.303R and log A, respectively.

Experimental

The reactions between $NaClO_3$, $FeSO_4$ and $NaHSO_3$ were conducted in a 1.0 L double-wall glass reactor with three inlets on the top. A stir set through the central inlet of the reactor was used to mix the reactants during the reaction. A thermometer passed through another inlet to measure the temperature in the reactor. The prepared reactant solutions were added through the additional inlet. A DL-501 thermostat was used to control the temperature in the reactor by circulating water around the reactor. Water and solutions of reactants $NaClO_3$, $FeSO_4$ and $NaHSO_3$ were prepared in advance and stored in separate vessels. All the chemicals used for the reactions and analysis of this study were analytical grade.

The concentrations of Cl^- during the reaction at different times were measured for monitoring the extent of reaction. To this end, the reactions in the reactor need to be stopped immediately after a desired period of reaction time. Sodium hydroxide solution (0.1 M) was prepared and used for that purpose, since the reaction between $NaClO_3$, $FeSO_4$ and $NaHSO_3$ stops when the pH of reaction 6 is higher than 7 [10]. The pH was monitored using a Fisher Scientific model 310 pH meter. Change of c_{Cl^-} was monitored for 240 seconds in each test. Rates for most non-zero and positive order reactions are higher at early times than later period; accordingly, a shorter sampling interval, 5 seconds, was chosen for the first 30 seconds of c_{Cl^-} monitoring time. This increased the density of the data points in the initial period of $c_{Cl^-} \sim t$ plots, where the $c_{Cl^-} \sim t$ curves typically appear steep, and thus improved the accuracy of curve fitted $c_{Cl^-} \sim t$ relationship. Ten seconds was used as the time interval for the remaining sampling period. Samples

were taken using pipettes. The value of c_{Cl^-} was determined using a Dionex Series 4000i ion chromatograph. The instrument was calibrated with a set of NaCl standard solutions at concentrations of 0, 50, 100, 150 and 200 ppm.

All the tests designed for the determination of reaction orders were conducted at 60 ºC. As previously mentioned, the initial concentration of the reactant for which the reaction order is to be determined should be much smaller than other reactants. Accordingly, 0.4425 mM $NaClO_3$, 88.5 mM $FeSO_4$ and 88.5 mM $NaHSO_3$ solutions were prepared and used for the determination of the reaction order of $NaClO_3$, 44.25 mM $NaClO_3$, 0.885 mM $FeSO_4$ and 88.5 mM $NaHSO_3$ solutions for the determination of reaction order of $FeSO_4$, and 44.25 mM $NaClO_3$, 88.5 mM $FeSO_4$ and 0.885 mM $NaHSO_3$ solutions for the determination of reaction order of $NaHSO_3$. The same volume (150 mL) of each prepared reactant solution (i.e., $NaClO_3$, $FeSO_4$, and $NaHSO_3$) was used in each reaction. Therefore, the real initial concentration of each reactant in each reaction was one third of that prepared before mixing.

Rate constants were calculated at different temperatures in order to determine the Arrhenius equation for reaction 6. To obtain the data needed for these purposes, 44.25 mM $NaClO_3$, 88.5 mM $FeSO_4$ and 88.5 mM $NaHSO_3$ solutions ($2\,c_{NaClO_3,0} = c_{FeSO_4,0} = c_{NaHSO_3,0}$) were prepared and used for reactions at 40 ºC, 50 ºC, 60 ºC, 70 ºC and 80 ºC. The concentrations of Cl^- generated, c_{Cl^-}, were measured 180 s after the reactions started. Rate constants at different temperatures were calculated using Equation 16.

RESULTS AND DISCUSSION

Synthesis of polymeric ferric sulfate from SO_2

Stoichiometric Model

Examination of the reactions proposed by Fan, *et al.* [11] gives some insight into the behavior of the basicity quality parameter. In this investigation, basicity of a batch was found to decrease linearly with time if the reaction was continued after the Fe(II) concentration approached zero. This behavior is shown in Figure 5. At that point the net

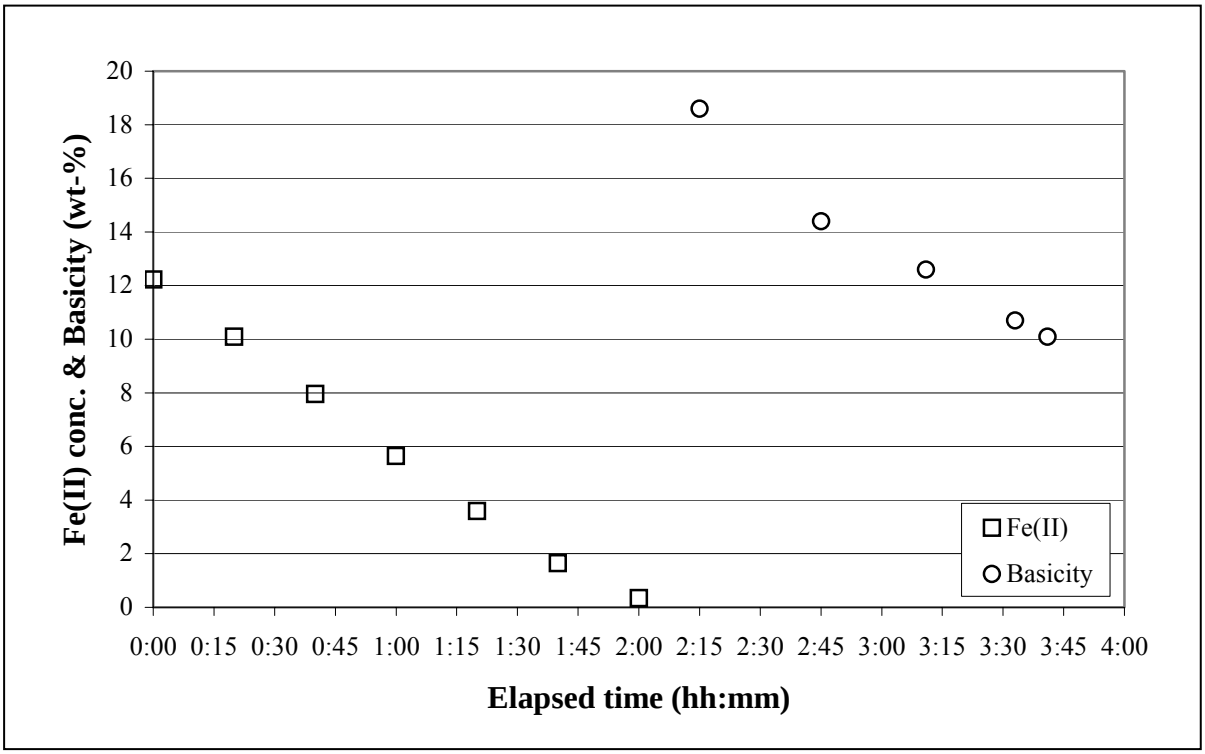


Figure 5. Decline of basicity after Fe(II) conversion is complete (temperature = 60.4 °C, oxidant dose = 0.61 g/min, SO_2 concentration = 5.4%, nitrogen flowrate = 1.2 lpm).

rate of the reaction in Equation (2) is near zero, allowing the acid produced in Equation (1) to accumulate in solution. The decreasing pH causes reduction in basicity seen in Figure 5. This is in agreement with the thermodynamic analysis given by Fan, *et al*. [11]. Therefore the amount of time that the SO_2 absorption was continued after all Fe(II) was converted allowed control of this parameter.

The iron measurements made during the course of the synthesis reveal that the initial Fe(II) concentration, equal at that point to the total iron, was greater than 10%. This was due to the fact that as the synthesis progressed, oxidant solution and SO_2 were added to the mixture, decreasing the total iron concentration toward an endpoint target of 10%. However, it was found that the conversion of Fe(II) to Fe(III) was completed before the stoichiometric quantity of SO_2 was added, with some variation depending on the rate of SO_2 absorption and oxidant dosing, as some of the protons required for this reaction were provided by the hydrolysis occurring. Thus, the synthesis required less SO_2 (and oxidant) than originally calculated. Based on this, the approximate composition of the PFS product solutions, assuming hydrolysis with n = 2, was as follows (by mass): 50% PFS (including all dissolved SO_x species), 48% water, and 2% sodium chloride.

A mole balance of the reactants is given in Table 4, showing that the rate of SO_2 absorption was 56.0% to 96.1% less than predicted by the reaction stoichiometry for the Fe(II) conversion rates found. A net accumulation of oxidant was also calculated by taking the oxidant input rate and subtracting the SO_2 absorption and Fe(II) conversion rates divided by their stoichiometric coefficients. It is a small negative quantity in all

Table 4. Reactant mole balances showing net oxidant accumulation and stoichiometric ratios.

Trial	SO_2 absorption rate[a] (mM/min)	Oxidant input rate (mM/min)	Fe conversion rate (mM/min)	Net oxidant Accumulation [b] (mM/min)	SO_2 deficit[c] (%)
1	0.797	5.634	37.681	-0.912	95.8
2	3.342	5.540	32.122	-0.928	79.2
3	2.321	5.634	34.036	-0.813	86.4
4	5.205	5.540	26.714	-0.647	61.0
5	0.791	5.728	40.327	-1.257	96.1
6	3.067	5.634	35.560	-1.315	82.8
7	2.132	6.479	35.096	-0.081	87.8
8	4.637	5.634	30.088	-0.927	69.2
9	0.761	1.878	10.576	-0.139	85.6
10	1.837	1.972	10.913	-0.459	66.3
11	1.649	1.784	8.302	-0.149	60.3
12	1.653	1.878	7.513	0.075	56.0
13	0.644	1.784	11.876	-0.410	89.1
14	1.412	1.784	10.013	-0.355	71.8
15	1.195	1.878	9.969	-0.182	76.0
16	1.516	1.878	8.566	-0.055	64.6

[a]Rate of SO_2 absorption calculated from concentration and removal efficiency measurements; [b]Net accumulation of oxidant in the reaction solution; [c]Percentage less than stoichiometrically predicted quantity of SO_2 absorbed

cases but one, supporting the proposed stoichiometric model if consideration is given to the net storage of SO_2 by the solution saturated with the gas. These calculations assume 10% total iron in the reaction solution, atmospheric pressure in the reactor, and gas flow rates measured at 20°C.

Factorial Analysis

To obtain trends and statistical results, average SO_2 removal efficiencies were calculated for each run by taking a mean of all the data points starting 30 minutes after the reaction began and running until the last Fe(II) data point was collected and the reaction was stopped. The initial 30-minute period was omitted from the average to allow the outlet gas concentration to stabilize after saturation of the solution and flushing of the headspace in the reactor and tubing. A linear regression was performed on the five

Fe(II) concentration values measured during the course of the reaction as well as one initial point calculated from the raw materials added to the reactor to find a concentration vs. time slope for each run. This slope was then used to calculate the rate of Fe(II) conversion for each run assuming the batch contained 10% Fe. The R^2 values for the linear fit were above 0.90 in all cases except one, and greater than 0.95 in most. These two values, average SO_2 removal efficiency and Fe(II) conversion rate, were taken as the quantitative results of each run to be used in the analysis. These values are shown in Table 5.

Due to limitations of the experimental apparatus, the data collected in this study does not allow clear separation of the effects of nitrogen flow rate and SO_2 concentration. Therefore, the SO_2 flow rate as pure SO_2, which is calculated from the nitrogen flow rate and SO_2 concentration, is given with the results in Table 5 and is useful to consider when looking at the behavior of the system.

Prior to undertaking the factorial test, the influence of the gas-liquid mass transfer rate was considered. A series of preliminary experiments showed evidence of a slightly higher SO_2 removal efficiency (on the order of 10%) with a fine-bubble fritted sparge when compared to an open 8 mm glass tube that released larger bubbles. This difference was ignored in the overall design of the experiment, and the open sparge was chosen for all subsequent tests due to problems with the fritted tubes clogging regularly under the conditions used in the factorial runs. Given the generally high solubility of SO_2 in water, as well as the fact that no quantitative kinetic models were derived from this investigation, the impact of the differences in SO_2 absorption between sparge devices on the results presented here is presumed to be minimal.

Table 5. PFS synthesis factorial conditions and results.

Tests	Ox. dose (g/min)	Temp (°C)	SO_2 conc. (%)	N_2 flow (l/min)	SO_2 dose (ml/min)	Fe conv. rate[a] (g/h)	SO_2 removal (% of inlet)
1	0.60	39.9	1.9	1.2	22.7	126.2	99.5
2	0.59	41.0	2.2	5.0	114.6	107.5	82.6
3	0.60	42.2	5.4	1.2	68.8	114.0	95.6
4	0.59	43.2	5.3	5.0	277.0	89.4	53.2
5	0.61	61.1	1.9	1.2	22.9	135.0	98.0
6	0.60	60.3	2.2	5.0	114.6	119.1	75.8
7	0.69	63.9	5.4	1.2	68.8	117.5	87.8
8	0.60	60.9	5.3	5.0	277.0	100.7	47.4
9	0.20	34.8	1.9	1.2	22.9	35.4	94.3
10	0.21	34.2	2.2	5.0	114.6	36.5	45.4
11	0.19	35.0	5.4	1.2	68.8	27.8	67.9
12	0.20	34.4	5.3	5.0	277.0	25.2	16.9
13	0.19	57.6	1.9	1.2	22.9	39.8	79.8
14	0.19	54.7	2.2	5.0	114.6	33.5	34.9
15	0.20	57.9	5.4	1.2	68.8	33.4	49.2
16	0.20	54.5	5.3	5.0	277.0	28.7	15.5
mid	0.30	47.6	3.7	3.1	117.3	51.2	46.9
mid	0.32	47.9	3.7	3.1	117.3	50.6	50.8
mid	0.31	47.0	3.7	3.1	117.3	49.9	50.0
mid	0.31	47.8	3.7	3.1	117.3	52.3	50.2
mid	0.31	47.6	3.7	3.1	117.3	48.2	51.3
r3	0.61	39.0	5.4	1.2	68.0	123.8	93.0
r8	0.62	59.0	5.3	5.0	277.0	107.1	47.5
r12	0.20	34.2	5.3	5.0	277.0	28.2	24.2
r16	0.22	56.4	5.3	5.0	277.0	31.7	18.0

Ox.-oxidizer; conc.-concentration; conv.-conversion.

Some trends are evident in the data. Foremost it can be seen that the oxidant dosing rate has the most profound effect on both the Fe(II) and SO_2 conversion. In addition, for a given temperature and oxidant dose, SO_2 removal efficiency is inversely proportional to the inlet SO_2 dose due to the oxidant being a limiting reagent. The data also suggest that some temperature effects may be present, which were investigated further and are discussed later in this section.

The statistical analysis for this study was based on 16 factorial runs, and five duplicates of one additional set of conditions near the midpoint of the factorial set. The

16 factorial runs were done in a randomized order, while the midpoints were made as a separate block following. In addition, a repetition of the first four runs was done after the midpoints to examine blocking effects in runs performed after the reactor was replaced due to failure of the drain valve following the final run of the 16 factorial runs. It was determined that blocking effects were not significant between the original and replacement reactors at the 5% level. Analysis of covariance was used to look for evidence of interaction of the reactor with the factors and treatments, and none was found at the 10% level.

Regression models were analyzed to investigate the effects involved between the factors. A model containing blocking, linear, quadratic, and two-way interaction effects (referred to as the full model) was found to give an R^2 value of 0.9852. It is given in Equation (18), where y is the predicted SO_2 removal efficiency, and the factors oxidant, temperature, sulfur dioxide, and nitrogen are abbreviated by O, T, S, and N, respectively. The terms ρ_1 and ρ_2 are intercepts for each reactor, and β_1 - β_4, β_5 - β_8, and β_9 - β_{14} are coefficients for the linear, quadratic, and two-way cross-product effects, respectively.

$$\begin{aligned} y = {} & \rho_1 \cdot 1_{[\text{reactor}=1]} + \rho_2 \cdot 1_{[\text{reactor}=2]} + \beta_1 O + \beta_2 T + \beta_3 S + \\ & \beta_4 N + \beta_5 O^2 + \beta_6 T^2 + \beta_7 S^2 + \beta_8 N^2 + \beta_9 OT + \\ & \beta_{10} OS + \beta_{11} ON + \beta_{12} TS + \beta_{13} TN + \beta_{14} SN \end{aligned} \qquad (18)$$

This model was compared to a reduced model containing only the blocking and linear effects using a lack-of-fit test. Despite the reduced model having an R^2 value of only 0.9494, it was found that the linear and quadratic terms did not contribute significantly to the full model. The analysis was then reconsidered by treating each of the 17 treatment combinations as classification variables, allowing the data to be analyzed in an ANOVA context (analysis of variance). In this way, the full model can be considered as a subset

of the ANOVA model, which had an R^2 value of 0.9978. Another lack-of-fit test performed between the ANOVA model and full model showed that there is still a significant amount of variance that is not explained by the full model, which is likely to lie in three- or four-way interactions between factors.

Given that the full model is not a significant improvement over the linear model, and that the full model resulted in a saddle point for the optimum factor combination, the results of the regression analysis were taken from the linear model, and are shown in Table 6. The parameter estimates indicate that a high dose of oxidant combined with low values for the other factors resulted in the maximum SO_2 removal efficiency. The absolute magnitude of the t statistic also gives an indication of the relative importance of the factor on the outcome. The fact that nitrogen flow rate appears to be relatively important is related to the effect of the total SO_2 dose, and not expected to be meaningful separately, as discussed above. Both the ANOVA analysis and the linear effects model indicate that maximum SO_2 removal occurs when oxidant concentration is high and the other three factors are low.

Table 6. Parameter estimates and statistics for linear regression model.

Parameter	Estimate	Standard Error	t value	$P_r > \lvert t \rvert$
block 1	61.08	1.72	35.55	< 0.0001
block 2	55.38	2.32	23.91	< 0.0001
oxidant	80.42	7.62	10.55	< 0.0001
temperature	-0.45	0.15	-3.09	0.0060
SO_2	-6.15	0.97	-6.34	< 0.0001
N_2	-9.45	0.81	-11.62	< 0.0001

Effect of Temperature on Synthesis Reactions

A series of data runs was performed at different temperatures, with oxidant and gas conditions held constant. SO_2 concentration was set at the 5% level, while nitrogen

flow rate was at 1 L/min, and oxidizer was dosed at 1-minute intervals. Results are shown in Figure 6. The rate of Fe(II) conversion increases with temperature, while SO_2

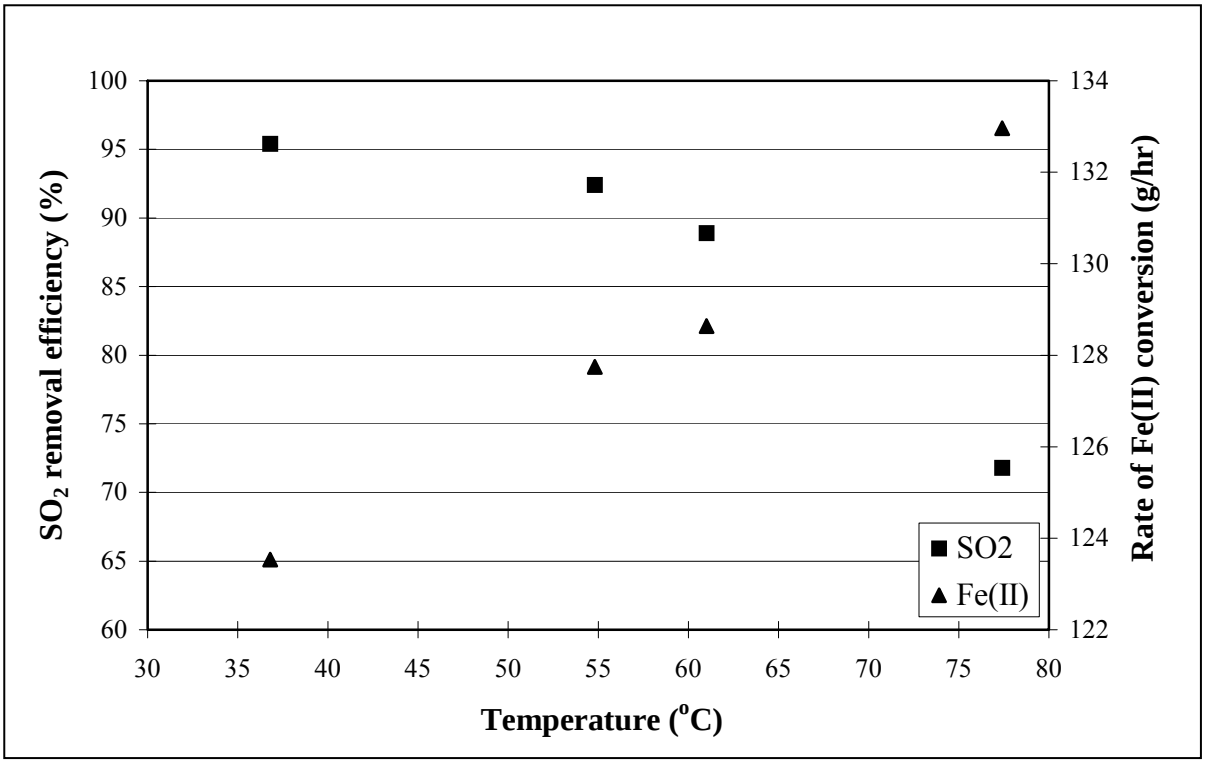


Figure 6. Effect of temperature on absorption rate of SO_2 and conversion rate of Fe(II) (SO_2 concentration = 5.4%, nitrogen flowrate = 1.2 L/min, oxidant dose = 0.60 g/min as $NaClO_3$).

removal efficiency decreases with temperature under the same conditions, most likely due to the faster Fe(II) reaction consuming more of the available oxidant. This effect is visible in runs 9-16 of the factorial tests where the amount of available oxidant is relatively low. This result suggests that the iron reaction is more sensitive to temperature than the SO_2 reaction, such that as the rate of iron conversion increases it consumes more of the oxidant, making less available for the oxidation of SO_2 and thereby reducing its absorption from the gas phase.

Characterization of Solid PFS

The results of the x-ray analysis of the three powder samples produced in the drying trials are shown together in Figure 7. The absence of any distinct peaks in the

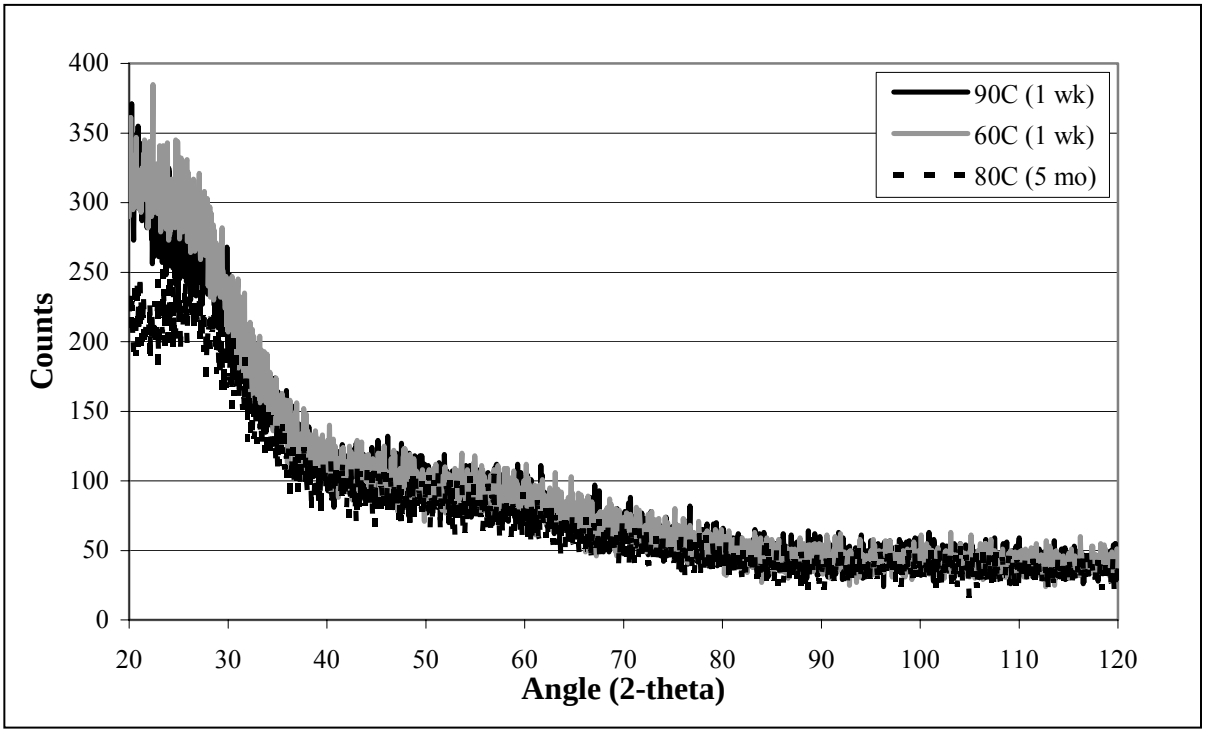


Figure 7. X-ray diffraction plot from solid PFS produced in the drying trials.

diffracted signals suggests that all the dried PFS powder is highly amorphous in nature [2]. A more amorphous solid PFS has been associated with better pollutant removals in bench-scale tests [2]. Very little difference was found between the samples, suggesting that the differences in drying temperature, basicity, and sample age described in Section 2.5 have little or no effect on the crystallinity of the solid PFS.

Laboratory Evaluation of PFS

Removal of Turbidity

Effect of Initial Turbidity of Kaolinite Suspensions

Polymeric ferric sulfate (B = 17.21 wt-%) from run 6 and FS solutions containing 11.0 wt-% (i.e., 1.98 M) total iron were used to conduct comparison coagulation tests over a dosage range from 0 to 0.046 mM in iron for low turbidity Kaolinite suspensions (10 NTU) and over a dosage range from 0 to 0.052 mM in iron with high turbidity suspensions (100 NTU) at pH 7.8. The results are plotted in Figure 8 and Figure 9, which show that PFS was more effective than FS in reducing the turbidity of either low or high turbid Kaolinite suspensions. For the low turbidity Kaolinite suspensions indicated in Figure 8, an abrupt change in residual turbidity occurred at 0.02 mM in Fe for both PFS and FS coagulants. When the coagulant dosage was below 0.02 mM in Fe, the turbidity removal efficiency was low, which may have been due to insufficient particle volume concentration in suspensions [2, 12]. However, when the coagulant dosages was greater than 0.02 mM in iron, the combined effects of Kaolinite particle destabilization and the increased particle volume from addition of coagulant led to good and substantial reduction of settled water turbidity. For high turbidity Kaolinite suspensions, Figure 9 shows that the greatest change in residual turbidity occurred with a coagulant dosage of 0.015 mM Fe, which was lower than the corresponding point in Figure 8 because of the higher particle volume concentration. Figure 8 indicates that even with higher dosages of coagulants, the residual turbidity, which is the residual turbidity in the supernatant after

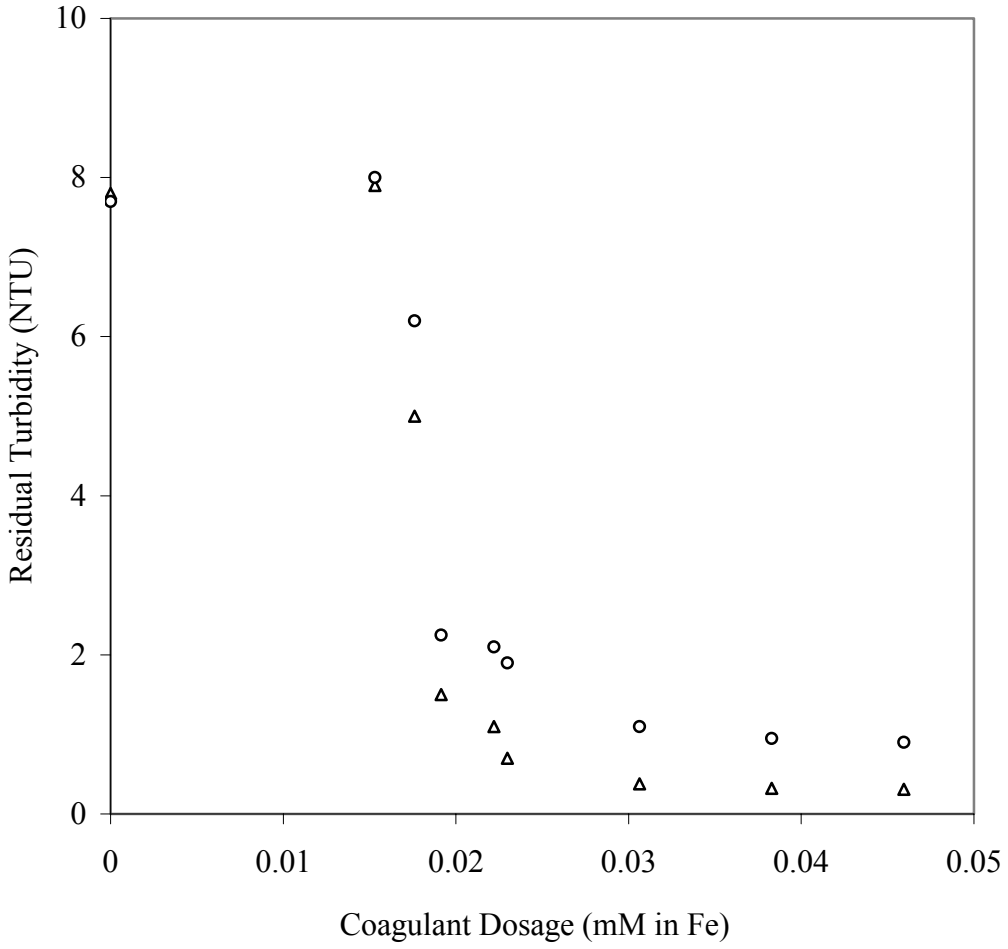


Figure 8. Comparison of polymeric ferric sulfate and ferric sulfate coagulation with low turbid Kaolinite suspensions (turbidity = 10 NTU, alkalinity = 45 mg/L as $CaCO_3$, initial pH = 7.8)

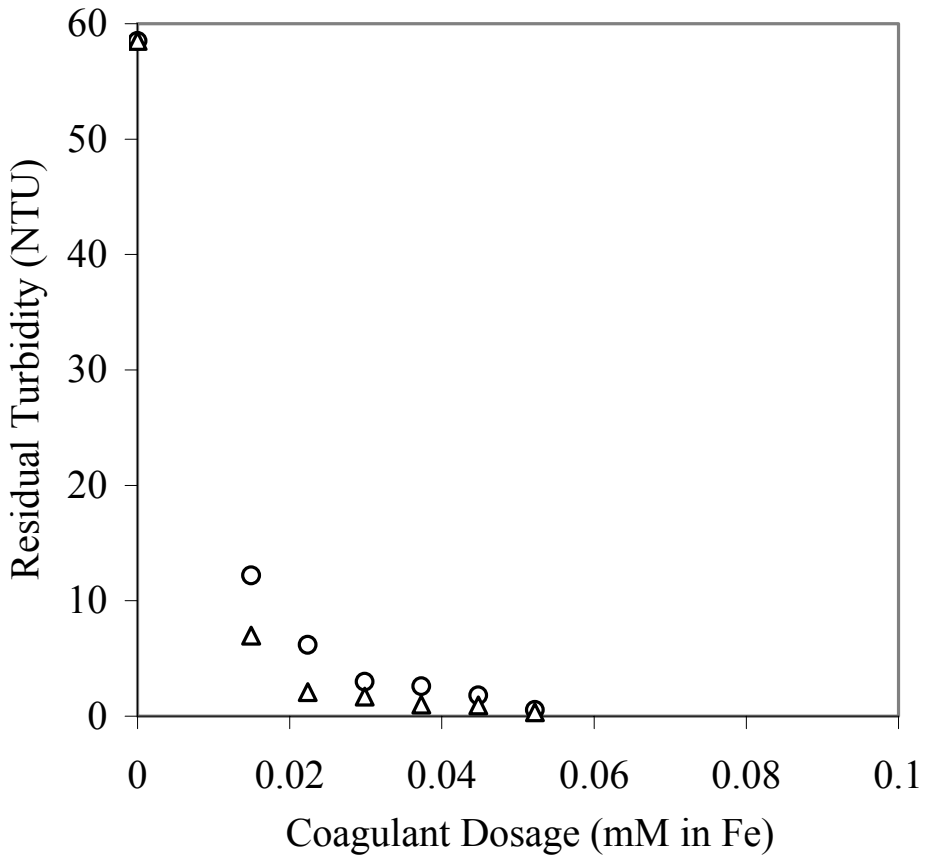


Figure 9. Comparison of PFS and FS coagulation performance with high turbid Kaolinite suspensions (turbidity = 100 NTU, alkalinity = 45 mg/L as $CaCO_3$, initial pH = 7.8)

30 minutes of settling, achieved with FS was never as low as that achieved with PFS. Figure 8 shows that with the same jar test conditions including a coagulant dosage of 0.03 mM in Fe a residual turbidity of 0.3 NTU was achieved with PFS while a residual turbidity of 0.9 NTU was achieved with FS. Figure 9 indicates that PFS is superior to FS in low dosage range for high turbidity Kaolinite suspensions.

Effect of kaolinite suspension pH

Results of jar tests with 10 NTU turbidity Kaolinite suspensions treated with PFS from run 6 or FS solutions in a pH range of 5.0 to 9.2 and with a coagulant dosage of 0.031mM in Fe are presented in Figure 10. These clearly illustrate that PFS is more effective than FS over most of pH range. The better performance of PFS may have been due to presence of preformed coagulant species, whereas chemical and physical conditions may have had to be appropriate for the production of effective coagulant species from FS. Low residual turbidities were observed with PFS over a pH range of 5.8 to 8.2 and with FS over a pH range of 6.5 to 8.2. The residual turbidities obtained with PFS and FS in the pH range of 6.5 to 8.2 were approximately 0.3 NTU and 1.1 NTU, respectively. The largest difference in residual turbidity achieved with PFS and FS occurred at pH 5.5. Furthermore, the PFS synthesized in this research seemed less effective above pH 8.5 than below. Above pH 8.5 the residual turbidity achieved with PFS was nearly the same as that achieved with FS. Finally, it was observed that after a coagulation test the pH of clarified water was always higher when PFS was used than when an equivalent dose of

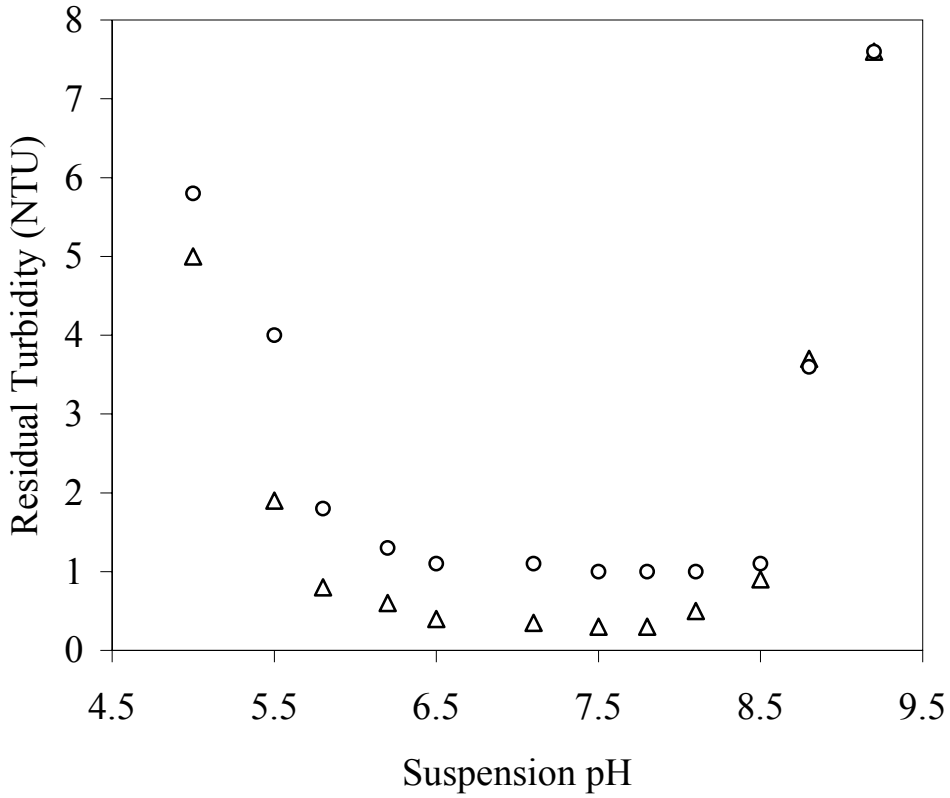


Figure 10. Comparison of PFS and FS coagulation performance with Kaolinite suspensions (turbidity = 10 NTU, alkalinity = 45 mg/L as $CaCO_3$, coagulant dosage = 0.031 mM in Fe) over an initial pH range of 5.0-9.2.

FS was used, which is significant due to the need to supply finished water with a pH of 8 or more to retard metal corrosion.

Effect of settling time

It was found during most jar tests that PFS formed flocs earlier than did FS. Furthermore, the flocs formed from PFS were larger than those formed from FS when the same dosages of coagulants were used. Based on this observation, we tested whether a suspension coagulated with PFS settled more quickly than one coagulated with FS. Jar tests were performed with 10 NTU Kaolinite suspensions using same dosage (0.031 mM in Fe) of the PFS from run 6 and FS solutions at pH 7.8; From the test results, we have found that the residual turbidity of a suspension coagulated with PFS reached 0.5 NTU and 0.37 NTU after 15 and 20 minutes of settling, respectively, while the lowest residual turbidity, obtained with FS, was 0.9 NTU observed after 25 minutes of settling. Therefore, PFS is a more efficient coagulant than FS from viewpoint of better floc formation and precipitation.

Effect of B value and structure of PFS

The effect of B value was evaluated through jar tests. The results, shown in Figure 11, reveal two features: first, the coagulation performance of PFS synthesized at either temperature increases with increasing B value until the B value reaches 18.76 wt-%; second, PFS synthesized at 55 °C performs better than PFS synthesized at 85 °C for a given B value. This result suggests that the amorphous structure of the PFS produced at the lower temperature may be more desirable than the crystalline structure of the PFS produced at the higher temperature.

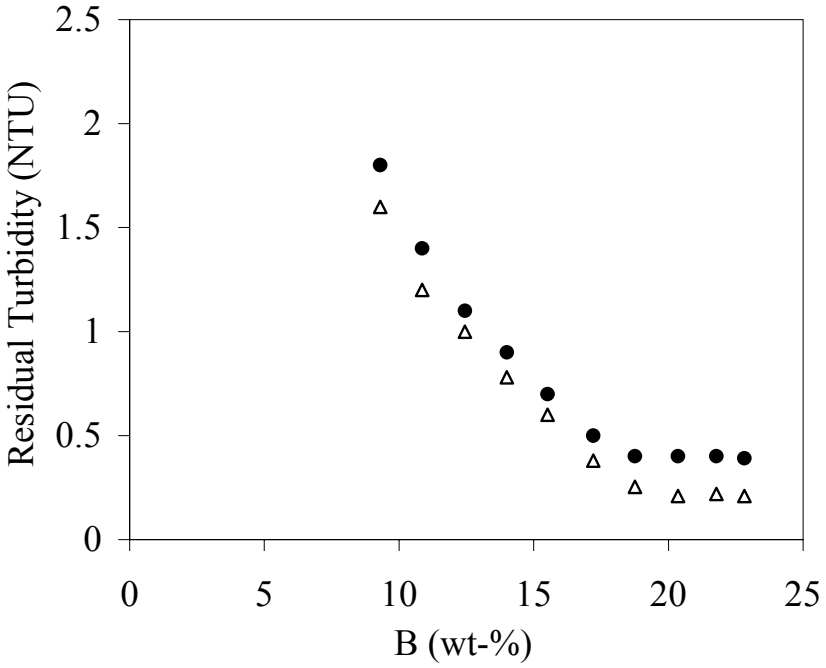


Figure 11. Effect of B value of PFS on coagulation of Kaolinite suspensions (turbidity = 10 NTU, alkalinity = 45 mg/L as $CaCO_3$, initial pH = 7.8, coagulant dosage = 0.031 mM in Fe).

Removal of Arsenic

The abilities of PFS and polymeric as well as conventional coagulants to remove arsenic were compared under different coagulation conditions, including initial pH, water temperature, type of coagulant, and application of coagulant aids. The results are described below.

Types of coagulants

Polymeric ferric sulfate (PFS) has been used to compare with polymeric ferric chloride, polymeric ferric sulfate, polymeric aluminum chloride, polymeric aluminum

sulfate, ferric chloride, ferric sulfate, aluminum chloride, and aluminum sulfate for As removal. Test results using PFS and coagulants are listed in Table 7. Results from corresponding iron-based coagulants are listed in Table 8.

Table 7. Removal of arsenic by aluminum-based coagulants (initial arsenic concentration = 50 μg/L, initial turbidity = 15.2 NTU, temperature = 23.5°C)

Initial pH of Suspension	Coagulant Dosage as Al (μM/L)	Removal of Arsenic (%)							
		due to Coagulation and Sedimentation				due to Coagulation, Sedimentation and Filtration			
		AS[a]	AC[b]	PAS[c]	PAC[d]	AS	AC	PAS	PAC
5.5	30	41.0	42.9	48.2	52.2	59.2	61.9	67.8	72.2
	50	69.6	70.6	78.2	82.2	86.2	87.6	93.9	97.3
	70	82.8	84.0	88.2	89.2	92.8	93.0	96.8	98.9
7.0	30	31.0	33.0	44.0	46.7	50.2	54.1	62.8	65.9
	50	59.4	60.8	72.2	75.6	72.3	74.9	84.9	86.8
	70	70.8	72.2	83.6	86.4	83.8	84.2	90.7	92.8
8.5	30	26.4	28.0	39.2	43.4	41.4	43.7	54.9	58.8
	50	54.2	55.9	67.0	71.1	69.2	68.8	79.2	82.7
	70	65.2	67.0	76.2	82.2	75.2	75.4	82.9	84.1

a-Aluminum Sulfate; b-Aluminum Chloride; c-Polymeric Aluminum Sulfate; d-polymeric Aluminum Chloride

Table 8. Removal of arsenic by iron-based coagulants (initial arsenic concentration = 50 μg/L, initial turbidity = 15.2 NTU, temperature = 23.5 °C)

Initial pH of Suspension	Coagulant Dosage as Fe (μM/L)	Removal of Arsenic (%)							
		due to Coagulating and Sedimentation				due to Coagulation, Sedimentation and Filtration			
		FS[a]	FC[b]	PFS[c]	PFC[d]	FS	FC	PFS	PFC
5.5	30	44.1	46.8	55.6	55.8	69.9	70.7	81.7	83.7
	50	72.0	73.7	92.7	92.9	97.2	97.3	98.6	99.0
	70	85.9	86.8	96.2	97.9	98.8	98.7	99.2	99.6
7.0	30	43.0	44.9	53.2	54.2	69.2	71.9	81.8	82.2
	50	71.6	72.6	90.8	92.2	90.2	91.6	98.0	98.3
	70	84.7	86.2	95.8	96.1	98.8	98.7	99.0	99.0
8.5	30	39.2	41.7	50.7	50.9	63.9	62.7	71.4	72.7
	50	67.2	68.6	87.6	87.8	83.0	84.3	88.6	89.2
	70	80.7	81.9	90.2	90.5	92.0	91.8	92.3	93.9

a-Ferric sulfate; b-Ferric chloride; c-Polymeric ferric sulfate; d-Polymeric ferric chloride

Table 7 reveals that, under the same initial conditions of suspension (i.e., arsenic concentration, turbidity, temperature), the efficiencies of the four aluminum-based coagulants, expressed as the percentage of arsenic removed follows the order: PAC ≥ PAS > AC > AS in the pH range of 5.5 to8.5. Furthermore, polymeric aluminum coagulants, including PAC and PAS, are superior to the conventionally applied AC and AS. As shown in Table 7, the highest arsenic removal efficiencies of PAC, PAS, AC, and AS before filtration are 89.2%, 88.2%, 84.0% and 82.8%, respectively, all occurring at an initial pH of 5.5. These results reflect the varying structures of these coagulants and different arsenic removal mechanisms. Polymeric aluminum coagulants contain species such as $[Al_2(OH)_2]^{4+}$, $[Al_3(OH)_4]^{5+}$, $[Al_8(OH)_{20}]^{4+}$,and $[Al_{13}O_4(OH)_{24}]^{7+}$ [13]. The relative concentrations of these species in PAC or PAS are functions of total aluminum concentration, the quantity of added sodium hydroxide or sodium bicarbonate during titration, rate of addition of the caustic, intensity of mixing, and aging condition of the preparation. The relative concentrations of these species also vary from one type of polymeric coagulant to another. For example, Smith and Martell [13] found that, thermodynamically stable (Al_{13}^{7+}) species, i.e., $[AlO_4(Al(OH)_2)_{12}]^{7+}$ in PAC but not in PAS. Rather they found $[Al_3(OH)_4]^{5+}$ as the predominant polymeric species in the PAS samples. Intuitively, strong coulombic forces appear to contribute to high arsenic (V) removal efficiencies of PAC and PAS as demonstrated in Table 7. The highly charged polymeric Al(III) species are stronger absorbents of arsenate ions—including $H_2AsO_4^-$, $HAsO_4^{2-}$, and AsO_4^{3-}—than the less-charged monomeric Al(III) species in AC or AS.

Anions and organic substances in water and coagulants may also affect the efficiency of arsenic removal. De-ionized water was used in this research, and no organic

substances were added to the test samples. We may therefore exclude the effects of anions and organics in raw water samples, and organics from coagulants on arsenic removal. As shown in Table 7, either SO_4^{2-} in PAS or AS, or Cl^- in PAC or AC, may explain differences in the level of arsenic removal between PAS and PAC, as well as between AS and AC. Negatively charged species in water decrease the removal of arsenic because they compete with $H_2AsO_4^-$, $HAsO_4^{2-}$, and AsO_4^{3-} for the surface complexation of preformed hydrous aluminum oxide (HAO). Therefore, the arsenic removal efficiency of PAS or AS is almost always lower than that from the same dosages of PAC or AC. This phenomenon is consistent with what was reported by Pierce and Moore [14] that at low arsenic concentrations, SO_4^{2-} is a stronger competitor than Cl^- for the adsorption of $H_2AsO_4^-$, $HAsO_4^{2-}$, and AsO_4^{3-} on hydrous aluminum oxide surfaces. NO_3^-, like Cl^- and SO_4^{2-}, had negative effect on the removal of As (V). However, NO_3^- was not a factor to cause the differences of arsenic removals among PAS, AS, PAC and AC when the initial pH values of arsenic suspensions are same due to the application of same dosage of HNO_3 in adjusting the pH of arsenic (V) suspensions.

PFC and PFS appear to exhibit better arsenic removal than PAC or PAS under most circumstances. As Table 8 illustrates, for the same initial turbidity, temperature and initial arsenic concentrations, the As(V) removal ability of the four iron-based coagulants in the pH range of 5.5 to 8.5 follows the order: PFC ≥ PFS > FC > FS. The highest arsenic removal efficiencies of PFC, PFS, FC, and FS before filtration are 97.9%, 96.2%, 86.8%, and 85.9%, respectively, at an initial pH of 5.5. The highly charged positive polymeric species such as $[Fe_2(OH)_2]^{4+}$, $[Fe_3(OH)_4]^{5+}$, and $[Fe_4(OH)_6]^{6+}$ may contribute to their greater arsenic removal efficiencies [15-17]. Moreover, due, probably, to the

different influences of Cl^- in FC and SO_4^{2-} in FS on the surface complexation of ionic groups of arsenic on hydrous ferric oxide (HFC), FC has a slightly higher arsenic removal efficiency than FS.

A comparison of Table 7 and Table 8 indicates that, in general, polymeric and conventional iron-based coagulants have greater arsenic removal abilities than corresponding polymeric and conventional aluminum-based coagulants. For example, for precipitation without filtration, the lowest arsenic removal efficiencies of AS and PAS at an aluminum dosage of 30 μM/L were 26.4% and 39.2%, respectively, while a comparable level of iron dosage in the form of FS and PFS increased arsenic removal efficiencies to 39.2% and 50.7%. Apparently, amorphous hydrous iron oxides having greater affinity toward As(V) than hydrous aluminum hydroxides, exhibit higher As(V) adsorptive capacity. Moreover, hydrous Fe(III) oxides are less soluble than hydrous Al(III) oxides, thus producing more solids for As(V) adsorption during coagulation process. Hering et al [18] reported that filtration with a 0.45 μm membrane can substantially remove fine particles from coagulant-treated water, consequently improve the removal of arsenic.

Results in Tables 7 and 8 indicate that high As(V) removals were achieved by using polymeric coagulants for coagulation. Under the given experimental conditions, filtration could not reduce As(V) removal concentration by more than 20%. The effects of filtration on arsenic removals were more obvious when dosages of coagulants were lower.

Coagulation Aid

Currently the water treatment industry uses activated silica to facilitate coagulation by forming negatively charged colloids, which help to increase the size of flocs and firm up the texture of aluminum and ferric hydroxides during coagulation. At appropriate dosages, these colloids can improve the turbidity removal efficiencies of different coagulants [19]. Based on this common practice, we investigated whether activated silica might have different effects on the arsenic removal abilities of polymeric and conventional coagulants during the coagulation process.

Figure 12 illustrates the arsenic removal rates of polymeric coagulants (PAS and PFS) and conventional coagulants (AS and FS), using activated silica as a coagulation aid in the dosage range of 0 to10 mg/L. At dosages of 2 mg/L, the net effect of activated silica on arsenic removal was negative for all four coagulants. However, the arsenic removal efficiencies of PAS, PFS, AS, and FS increased for dosages from 2 to 10 mg/L. Due to the formation of larger and tougher flocs, in this range activated silica was clearly superior to monomeric silicic species, i.e., $H_2SiO_4^{2-}$ and $H_3SiO_4^{-}$ for reducing residual turbidity, and thus enhancing the removal of arsenic through adsorption on the surface of hydrous aluminum or iron oxide [14]. The flocs formed by PAS, PFS, AS, and FS, in the presence of activated silica (at 6 mg/L) were larger and tougher, and settled more quickly and steadily. Therefore, it is expected that AS with activated silica as coagulation aid, can achieve a lower residual turbidity and a high arsenic removal rate. This is in accordance with findings reported by Hathaway and Rubel [20] as shown in Figure 12. Furthermore, when dosages of activated silica reached the ranges of 6-10 mg/L and 8-10

mg/L, the net effects on the arsenic removal efficiency of polymeric coagulants (PAS and PFS) and conventional coagulants (AS and FS) were still positive but began to

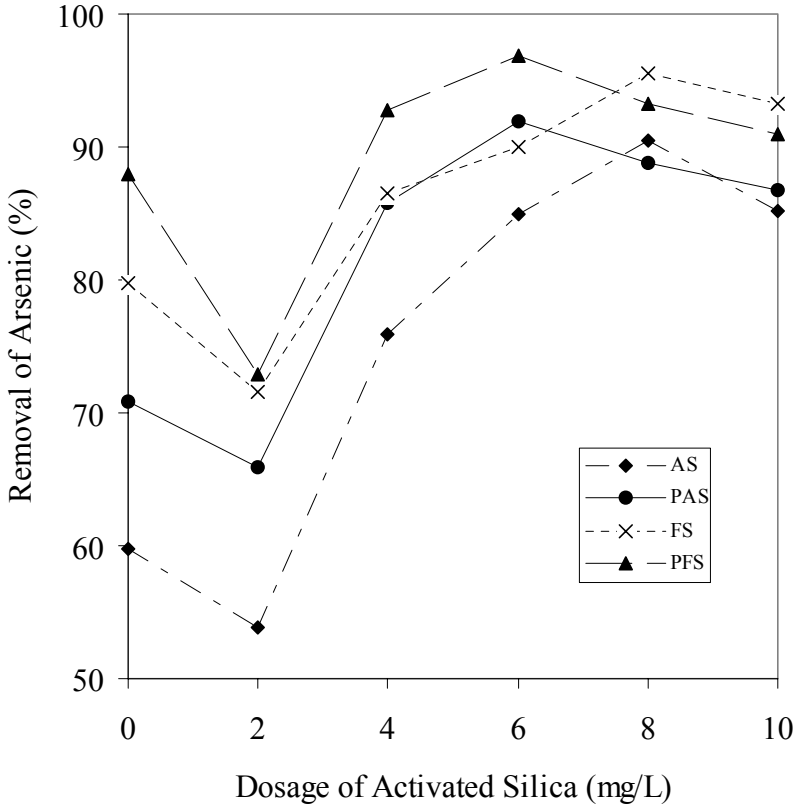


Figure 12. Effect of adding activated silica on removal of arsenic (initial arsenic concentration = 50 μg/L, initial pH of suspension = 7, dosage of coagulants = 35 μM as Al for AS or PAS, 35 μM as Fe for FS or PFS, T = 23.3 °C, after filtration).

diminish, due to the increased competition between monomeric silicic species such as $H_2SiO_4^{2-}$ and $H_3SiO_4^-$ SiO_3^{2-} with arsenic for adsorption on the surfaces of hydrous aluminum or iron oxides. Overall, among the four coagulants tested, the polymeric coagulant PFS was the least affected by the addition of activated silica for the removal of arsenic; the conventional coagulant AS was the most affected.

Initial pH of Suspension

Tables 7 and 8 display the results of arsenic removal using the same dosages of coagulants (based on Al or Fe concentration) over a initial pH range of 5.5 to 8.5 in the presence of polymeric (PAC, PAS, PFC, and PFS) or conventional (AC, AS, FC, and FS), Fe and Al coagulants. Results clearly indicate that pH affects the efficiency of arsenic removal.

As Table 7 demonstrates, when initial pH increased from 5.5 to 8.5, the As(V) removal efficiency of AS and AC decreased by 15 and 17% respectively, at an Al dosage of 30 μM/L and 70 μM/L. It is also interesting to note that PAS and PAC are less pH-dependent than AS and AC with respect to arsenic removal. Moreover, results in Table 5 also indicate that between initial pH 7 and 8.5 and without filtration, neither AS or AC can attain arsenic removal efficiencies higher than 80% (i.e., equivalent to higher than 10 μM/L residual arsenic at an initial arsenic concentration of 50 μM/L). Therefore, when applied in high pH water, conventional aluminum coagulants clearly will not be able to meet new EPA arsenic standard of 10 μM/L. Consequently, coagulation aids may be necessary when using conventional aluminum coagulants for As(V) remove arsenic from high-pH water.

Results in Table 8 reveal that changing the initial pH do not affect the arsenic removal efficiency of FS, FC, PFS and PFC as much as that of aluminum-based coagulants. When the initial pH was increased from 5.5 to 8.5, and under the same coagulant dosages, the arsenic removal efficiency of all polymeric and conventional iron coagulants increased from 1-6% to 1-14%, respectively, both with and without the aid of filtration.

Temperature

Figures 13 and 14 show that effects of temperature on the arsenic removal

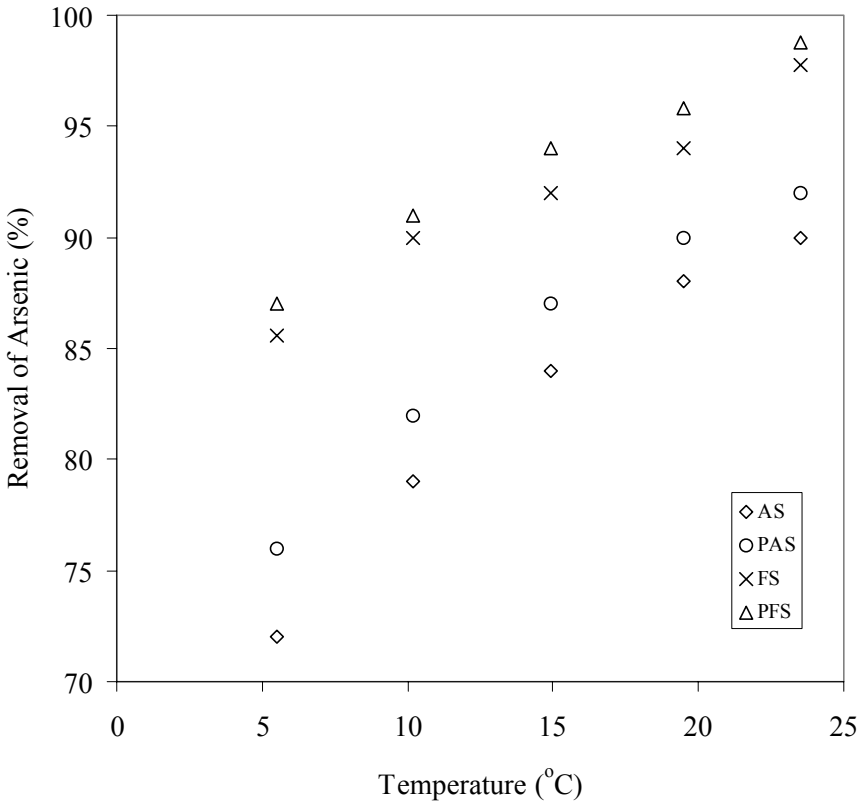


Figure 13. Effect of temperature on arsenic removal (initial arsenic concentration = 50 μg/L, initial turbidity = 15.2 NTU, initial pH of suspension = 7, coagulant dosage = 70 μM as Al or Fe, after filtration).

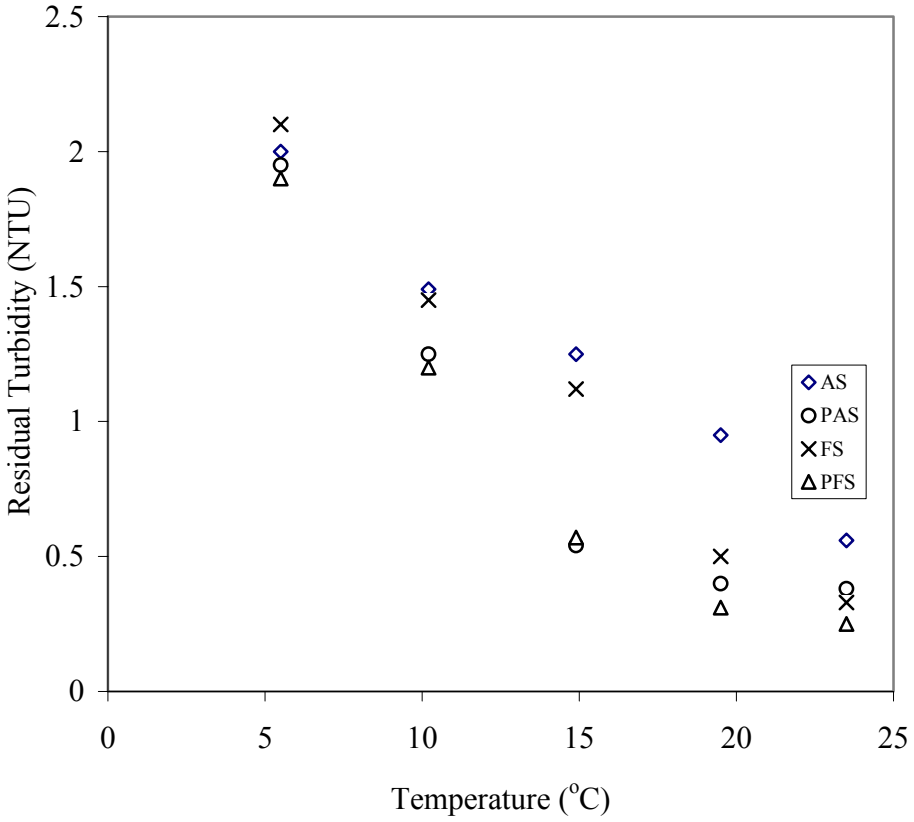


Figure 14. Effect of temperature on removal of turbidity (initial arsenic concentration = 50 μg/L, initial turbidity = 15.2 NTU, initial pH of suspension = 7, coagulant dosage = 70 μM as Al or Fe, before filtration).

efficiency and residual turbidity of waters treated by polymeric coagulants (PAS, PFS) and conventional coagulants (AS, FS). The general trend in Figures 13 and 14 suggests that arsenic removal efficiency and residual turbidity improve with temperature increased from 5.5 to 23.5°C, under otherwise identical experimental conditions. The arsenic removal efficiency of AS and PAS after filtration increased about 23%, while that of FS and PFS improved about 15%; the residual turbidity of treated water before filtration decreased about 1.5 NTU when water temperature was increased from 5.5 to 23.5 °C.

Although the differences in arsenic and turbidity removal capabilities are small between PFS and AS at the two temperature extremes, i.e., 5.5 and 23.5 ^{o}C, PFS is a clearly stronger coagulant than FS over most temperature range studied. Consequently, it is a better coagulant than FS thereby a better reagent for As(V) removal d extreme temperature point 5.5. Furthermore, a comparison of Figures 13 and 14 reveals that, even the residual turbidity of treated waters is similar at lower temperatures, the arsenic removal efficiencies of AS, PAS, FS and PFS are significantly different.

Initial Concentration of Arsenic (V)

Figure 15 shows the effect of initial arsenic concentration on its removal. Results

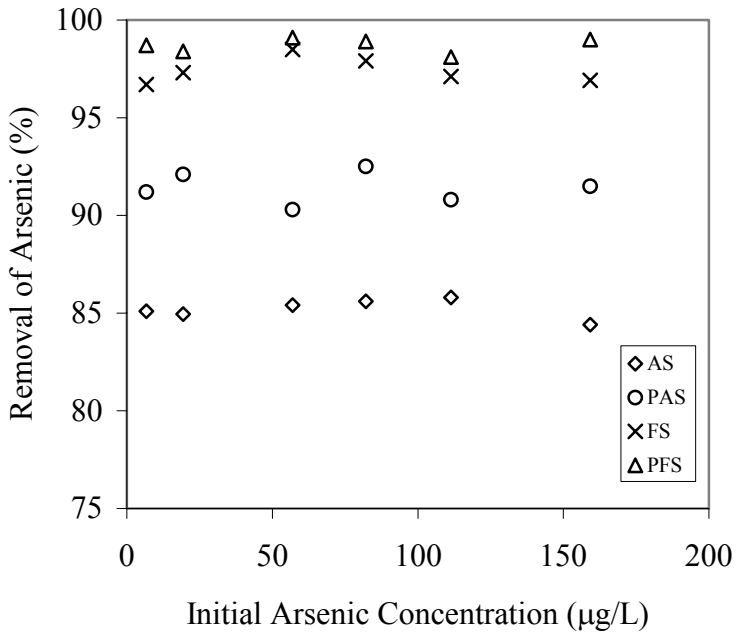


Figure 15. Effect of initial arsenic concentration on arsenic removal (initial turbidity = 14.2 NTU, initial pH of suspension = 7, coagulant dosage = 70 μM as Al or Fe, T = 23.5 °C, after filtration).

indicate that when the initial As(V) concentration increased from 6 to 160 μg/L, the As(V) removal efficiency varied within 1 to 2%. Therefore, under the experimental conditions of this study, the initial arsenic concentration plays an insignificant role on As(V) removal exemplified by AS, PAS, FS, and PFS.

Pilot-Scale Evaluation of PFS

Test in Des Moines Water Works

The pilot study looked primarily at turbidity and disinfection byproduct precursor removal. Other water quality parameters such as alkalinity, temperature, and pH were also measured. Due to the nature of the water supply to the pilot plant, raw water quality varied significantly between runs and during the course of each run. Therefore, rather than repeatable quantitative results, trends were identified.

Over the course of the study period, the temperature of the raw water was 28-30°C and its pH varied between 7.6 and 7.9. Turbidities at the three stages of treatment, as well as overall removal efficiencies for the six agent-dose combinations, are shown in Table 8. The turbidity figures given are an average of six hourly measurements. Although PFS appears slightly more effective at the lowest dose, the turbidity removal capabilities of PFS and FC are not shown to differ greatly in this study (more studies are in order to explore this). It was noted by the plant operators that, in comparison to FC, PFS produced a floc that was larger, less dense, and slower to settle. Initial and final alkalinities are also given in Table 9, in mg/l as $CaCO_3$, with corresponding consumption

Table 9. Pilot study turbidity and alkalinity removal results (raw water temperature = 28-30°C, pH = 7.6-7.9).

	2 mg/L		3 mg/L		4 mg/L	
	PFS	$FeCl_3$	PFS	$FeCl_3$	PFS	$FeCl_3$
(1)	(2)	(3)	(4)	(5)	(6)	(7)
Raw water NTU	17.5	15.1	14.5	14.1	14.1	14.0
Pre-sediment NTU	5.0	4.3	5.2	3.3	3.8	4.3
Pre-filter NTU	2.0	3.0	2.9	1.5	2.4	1.7
NTU reduction	88.6%	80.1%	80.0%	89.4%	83.0%	87.9%
Raw water alkalinity (mg/l)	167	163	166	171	169	169
Pre-filter alkalinity	68	63	70	53	55	57
Alkalinities consumption	59%	61%	58%	69%	67%	66%

rates. Raw water alkalinities were fairly consistent throughout the trials, and the data shows that, in general, PFS did consume less alkalinity than FC during the treatment process. Table 10 shows removal data for TOC (mg/l), DOC (mg/l), and UV-254 (AU) disinfection byproduct precursors for the same agent-dose combinations. TOC removal was higher with PFS at 3 mg/L and 4 mg/L, while the removal of DOC was greater with PFS at 2 mg/L and 3 mg/L. UV-254 removal was higher with PFS at all three dosages.

Table 10. Disinfection byproduct precursor removal in pilot study (raw water temperature = 28-30°C, pH = 7.6-7.9).

	2 mg/L		3 mg/L		4 mg/L	
	PFS	$FeCl_3$	PFS	$FeCl_3$	PFS	$FeCl_3$
(1)	(2)	(3)	(4)	(5)	(6)	(7)
Raw water TOC (mg/l)	4.96	5.71	5.95	5.80	6.23	5.44
Pre-filter TOC	2.39	1.95	2.16	2.07	2.01	2.01
TOC reduction	51.8%	65.9%	63.7%	64.3%	67.7%	63.0%
Raw water DOC (mg/l)	3.04	3.08	3.41	2.75	3.33	3.60
Pre-filter DOC	1.80	2.17	2.12	2.11	2.01	2.01
DOC reduction	40.8%	29.6%	37.8%	23.3%	39.6%	44.2%
Raw water UV-254 (AU)	0.104	0.077	0.130	0.072	0.178	0.127
Pre-filter UV-254	0.036	0.072	0.049	0.046	0.046	0.041
UV-254 reduction	65.4%	6.5%	62.3%	36.1%	74.2%	67.7%

Tests in Savannah Industrial and Domestic (I&D) Water Treatment Plant

Polymeric ferric sulfate (PFS) was compared with other iron-based coagulants and alum in the pilot plant tests. The average coagulant dosage and mixed water pH for the experimental runs are summarized in Table 11. Although, the water quality changed

Table 11. Coagulant dosage and pH comparisons

	Averaged Experimental Run Conditions					
	PFS		Ferric Chloride		Ferric Sulfate	
	Alum	PFS	Alum	Ferric Chloride	Alum	Ferric Sulfate
Dosage, mg/L	48	65	45	40	46	110
Average pH	5.4	4.0	5.73	4.7	5.7	4.02

between experimental runs some information regarding the dosage required to achieve effective turbidity removal in comparison to alum can be obtained. The alum dosage for the three experimental runs was consistent at an average concentration of about 46mg/l. Ferric sulfate required the highest average dosage in comparison to alum while ferric chloride required the lowest average dosage for effective treatment. The iron-based coagulants resulted in a much lower mixed water pH in comparison to the alum coagulant with the PFS and ferric sulfate reducing the pH to approximately 4.0.

As shown in Figure 16 greater reductions in TOC and total suspended solids (TSS) are observed with PFS than with alum. However, alum produces greater reductions in nitrate, iron, and total dissolved solids (TDS). Ironically, the aluminum residual when using PFS increases 137% compared to an increase of only 61% when using alum. In addition, water treated with PFS shows a greater increase in specific conductance when

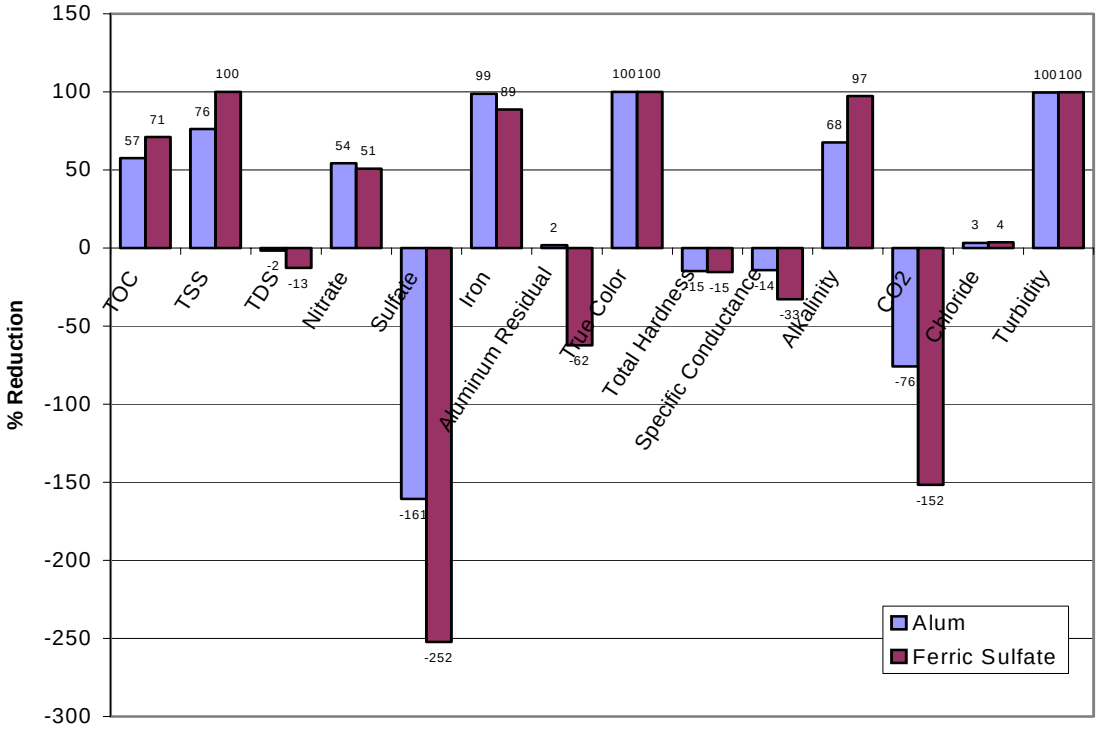


Figure 16. Comparison of ferric sulfate and alum in Savannah Industrial and Domestic Water Treatment Plant.

compared to water treated with alum. All of the alkalinity was removed from the water when using PFS as the coagulant while 24% of the initial alkalinity remains when using alum. The CO_2 increases by 75% when using alum compared to an increase of 173% when using PFS as the coagulant. The sulfate concentration increased when using both coagulants, however, no initial concentration of sulfate could be measured and therefore the percentage increase could not be effectively calculated. The sulfate concentrations increased from a value of zero to average values of 27.9 and 39.7 mg/l for alum and PFS, respectively.

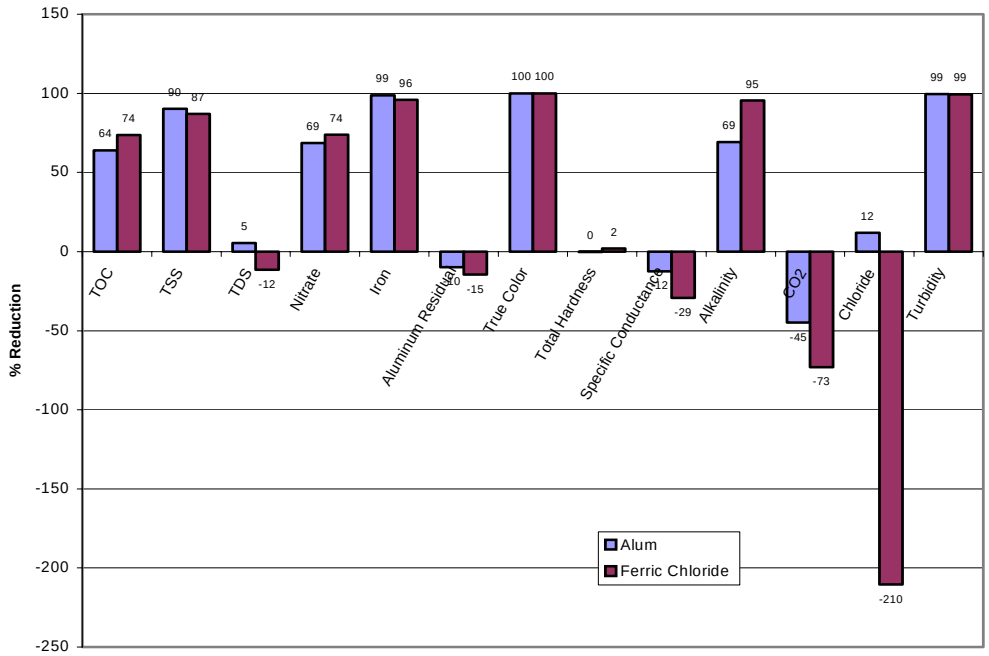


Figure 17. Comparison of ferric chloride and alum in Savannah Industrial and Domestic Water Treatment Plant.

Figure 17 shows a greater reduction in TOC and nitrate with ferric chloride as opposed to alum. However, slightly greater reductions in TSS and iron are observed when using alum as the coagulant. A reduction in TDS of 5 % is observed when using alum as the coagulant in comparison to an increase of 12% when using ferric chloride as the coagulant. The aluminum residual for the two coagulants shows a greater increase at 15% for the ferric chloride in comparison to a 10% increase with alum. Nearly 95% of the alkalinity is removed from the water when using ferric chloride as opposed to 75% reduction observed when treating with alum. In addition, a reduction in chlorides is observed when using alum in comparison to an increase of nearly 210% observed when

using ferric chloride. The sulfate concentration (which is not shown on the figure) increased for water treated with both coagulants. Water treated with alum showed the greatest increase, increasing from a value of 1.6 mg/l in the raw water to a value of 27.1 mg/l in the filtered water (1593 % increase). While water treated with ferric chloride showed an increase from 1.6 mg/l to a value of 6.6 mg/l (312% increase). A greater increase in specific conductance is observed in water treated with ferric chloride than that observed when using alum as the coagulant.

In comparison of the results acquired when using ferric sulfate and PFS the results are very similar. Both coagulants cause a greater reduction in TOC and TSS when compared to that achieved in alum. Greater reductions in nitrate and iron are achieved with alum in a comparison of PFS and ferric sulfate with alum. Greater increases in specific conductance and CO_2 as compared to alum are observed in PFS in comparison to ferric sulfate.

Increases in both sulfate and aluminum after treatment were seen with all of four of the coagulants, coupled with the observance of higher specific conductance and lower TOC. This indicates that both sulfate and aluminum are present in the raw water as organically bound species, and therefore undetectable by the methods used. The treatment process results in the reduction of the organic matter and destruction of the complexes. The ligands are then detected as ionic species, resulting in higher sulfate and aluminum concentrations as well as a higher specific conductance. The lower pH required for all of the iron-based coagulants would favor the dissolution of the complexed species. This coupled with the presence of sulfate in the iron-based coagulants results in significantly higher sulfate concentrations in the treated water than that of the raw water.

Evaluation of corrosion

Electrochemical explanation.

When the metal specimens were immersed into the coagulant solutions, an electrochemical reaction took place with the metal acting as an anode and the impurities within metal as a cathode. This reaction then resulted in the loss of metal in the anode reaction, and hydrogen gas generation in the cathode reaction. The electrochemical reactions involved in the corrosion are as shown with reactions (19) and (20) [21],

$$Fe + 2H^{+} \longrightarrow Fe^{2+} + H_2 \quad E_0 = 0.44V \tag{19}$$

$$2Al + 6H^{+} \longrightarrow 2Al^{3+} + 3H_2 \quad E_0 = 1.68V \tag{20}$$

Apart from these two electrochemical reactions, redox reaction also played an important role in the corrosion behavior. The ferric chloride (FC) solution containing 10 wt% Fe(III) boiled within 10 minutes of immersing the aluminum specimens. The temperature increased rapidly from 20 °C to higher than 100 °C. After the reaction was finished, solution samples were analyzed for Fe(II) and Fe(III). The solution contained 10 wt% Fe(II) and 0 wt% Fe(III); obviously, all of the Fe(III) was converted into Fe(II) through the reaction.

According to ΔG values of the redox reaction that may take place, the reaction can proceed during all the test periods. For the aluminum case, the concentration of Al(III) and Fe(II) at the beginning of the reaction was negligible compared to the Fe(III)concentration, which made ΔG of reaction 21 negative [22]. For the reaction to stop proceeding to the right, the concentration of Fe(III) will almost be negligible. That means Fe(III) can be virtually completely reacted if enough aluminum is provided. For the steel case, Fe(II) was negligible at the beginning of reaction. Fe(III) should be much

lower than Fe(II) to make the reaction stop, which means all Fe(III) is almost completely consumed if enough steel is provided for reaction 22 [21-22]. In both cases, redox reaction will happen as long as the metals and coagulants exist in the solution.

$$Al + 3Fe^{3+} \longrightarrow Al^{3+} + 3Fe^{2+} \quad E^0 = 2.45V$$

$$\Delta G = \Delta G_f^0 + RTlnQ = -169.1 + 1.99 \times 10^{-3} T \ln \frac{\left[Al^{3+}\right]\left[Fe^{2+}\right]^3}{\left[Fe^{3+}\right]^3} \qquad (21)$$

$$Fe + 2Fe^{3+} \longrightarrow 3Fe^{2+} \quad E^0 = 1.21V$$

$$\Delta G = \Delta G_f^0 + RTlnQ = -58.8 + 1.99 \times 10^{-3} T \ln \frac{\left[Fe^{2+}\right]^3}{\left[Fe^{3+}\right]^2} \qquad (22)$$

Effects of Temperature

Test results showed that temperature had a substantial influence on corrosion: the higher the temperature, the higher the weight loss in the metal specimens. For the case of a steel specimen immersed in a PFS solution containing 10 wt% Fe(III) for 10 hours, the specimen's weight loss at the temperature of 65 °C was 6.8686 g, about twenty-two times higher than that at 5 °C, which was only 0.3032 g.

Figure 18 illustrates the relationship between corrosion weight change and temperature. When the temperature was increased, the corrosion rates increased dramatically in all reaction system. The reaction rates at 65 °C in some systems, such as steel immersed in PFS solution containing 1 wt% and 10 wt% Fe(III), however, were not as high as those expected from the trend obtained from the previous four corrosion rates

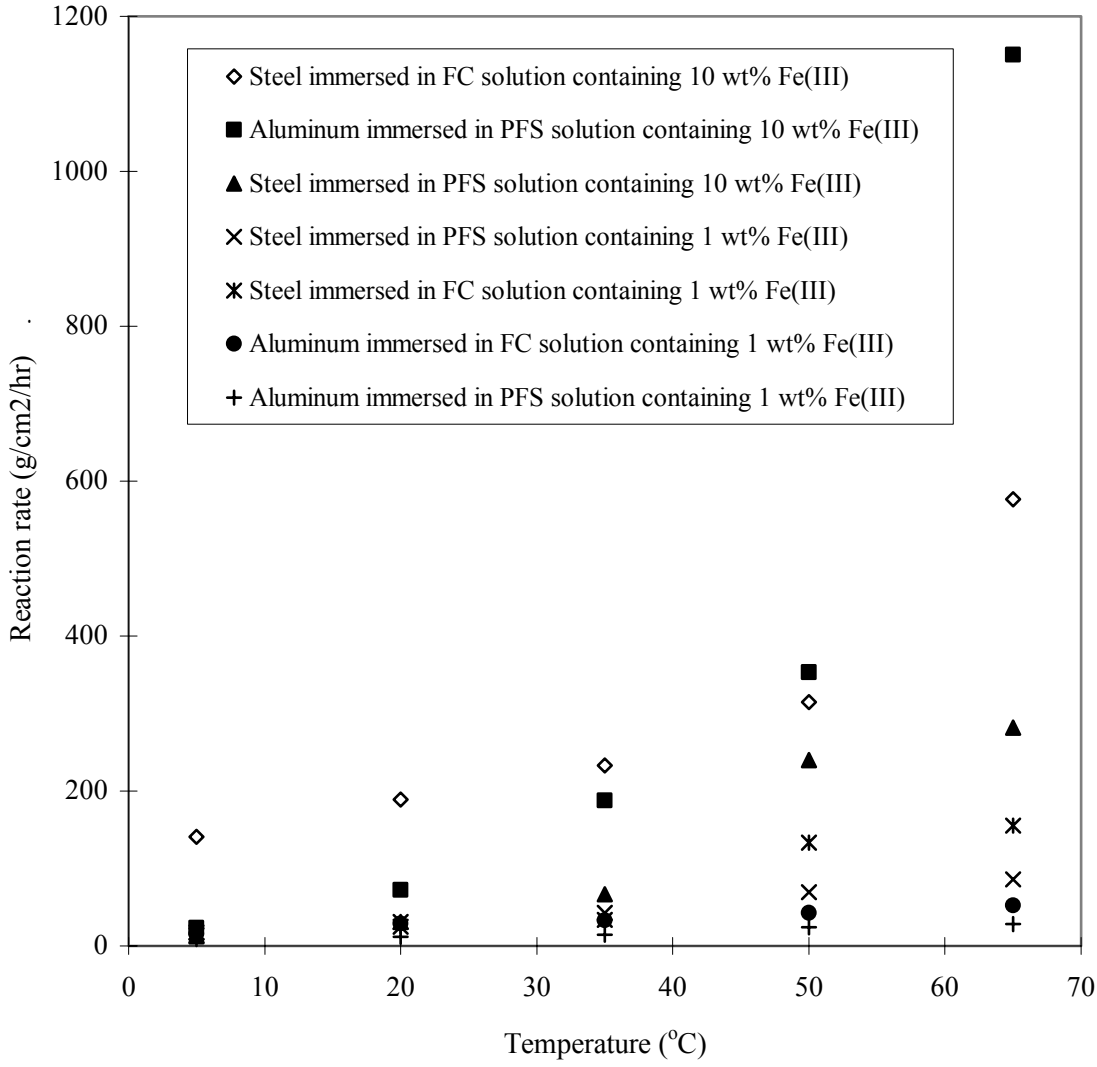


Figure 18. The effect of temperature on reaction rate

at lower temperatures. That may be explained by the tendency of PFS to more easily subject to hydrolyzation at higher temperatures than FC solutions containing the same concentration of Fe(III) [10], which was shown as in reaction 23:

$$Fe^{3+} + 3H_2O \longrightarrow Fe(OH)_3 + 3H^+ \qquad (23)$$

The hydrolyzation resulted in a decrease of Fe(III) concentration in solution. Consequently, the reaction rate between iron and Fe(III), a major reaction that caused the

corrosion of the steel specimen, was also inhibited caused by ΔG approaching to zero, which means the termination of reaction. For steel immersed in an FC solution containing 10 wt% Fe(III) (Figure 19), the reaction proceeded smoothly when the

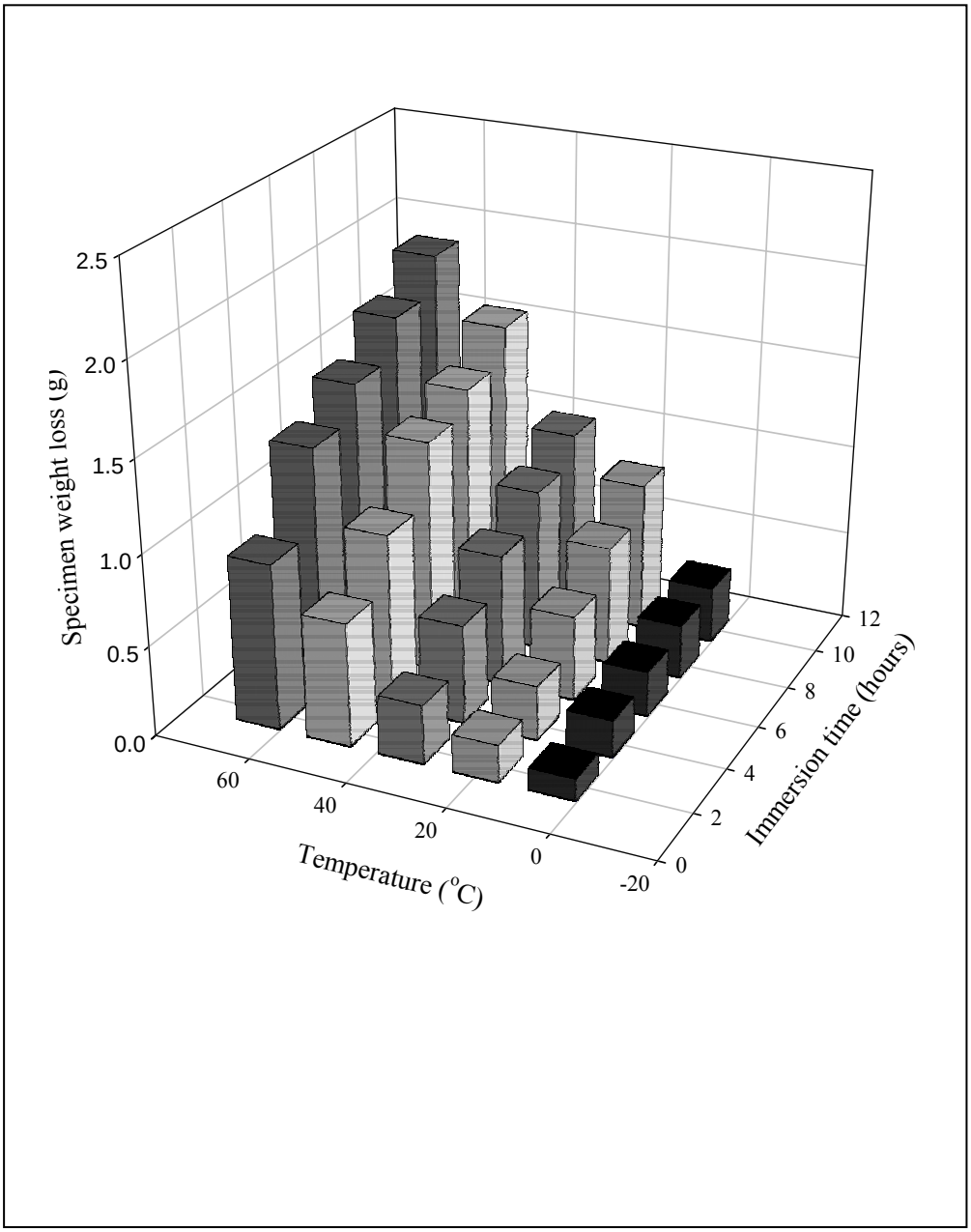


Figure 19. Steel specimen immersed in PFS solution with 1 wt% Fe (III)

temperature was below 65 °C. However, the reaction became rather furious accompanied with lots of bubbles produced and temperature increase caused by heat accumulation through reaction.

Effect of concentration

The corrosion rates increased with the increase of solution concentration. At temperature of 5 °C, the corrosion rate of the steel specimens in the FC solution containing 10 wt% Fe(III) was 140 g/cm^2.hr, while the corrosion rate in the FC solution containing 1 wt% Fe(III) was only 17 g/cm^2.hr. When the temperature increased to 65 °C, the corrosion rates of the steel specimens in these two solutions were 576 g/cm^2.hr and 155 g/cm^2.hr, respectively. For the aluminum specimens, the corrosion rates were 23 g/cm^2.hr and 9 g/cm^2.hr in the PFS solutions containing 10 wt% and 1 wt % Fe(III) at the temperature of 5 °C. When the temperature was increased to 65 °C, the corrosion rates changed to 1150 g/cm^2.hr and 28 g/cm^2.hr. The reaction rates in the PFS solution containing 10 wt% Fe(III) were 4000% higher than reaction rates in solutions containing 1 wt% Fe(III). When the aluminum was immersed in an FC solution containing 1 wt% Fe(III), the weight loss was 0.7773 g. The corrosion rate of aluminum in the FC solution containing 10 wt% Fe(III) was much higher. However, the rate was unable to be determined since the aluminum specimens were completely corroded in 15 minutes. Obviously, higher concentration solutions are more corrosive than lower concentrations (Figures 20 and 21).

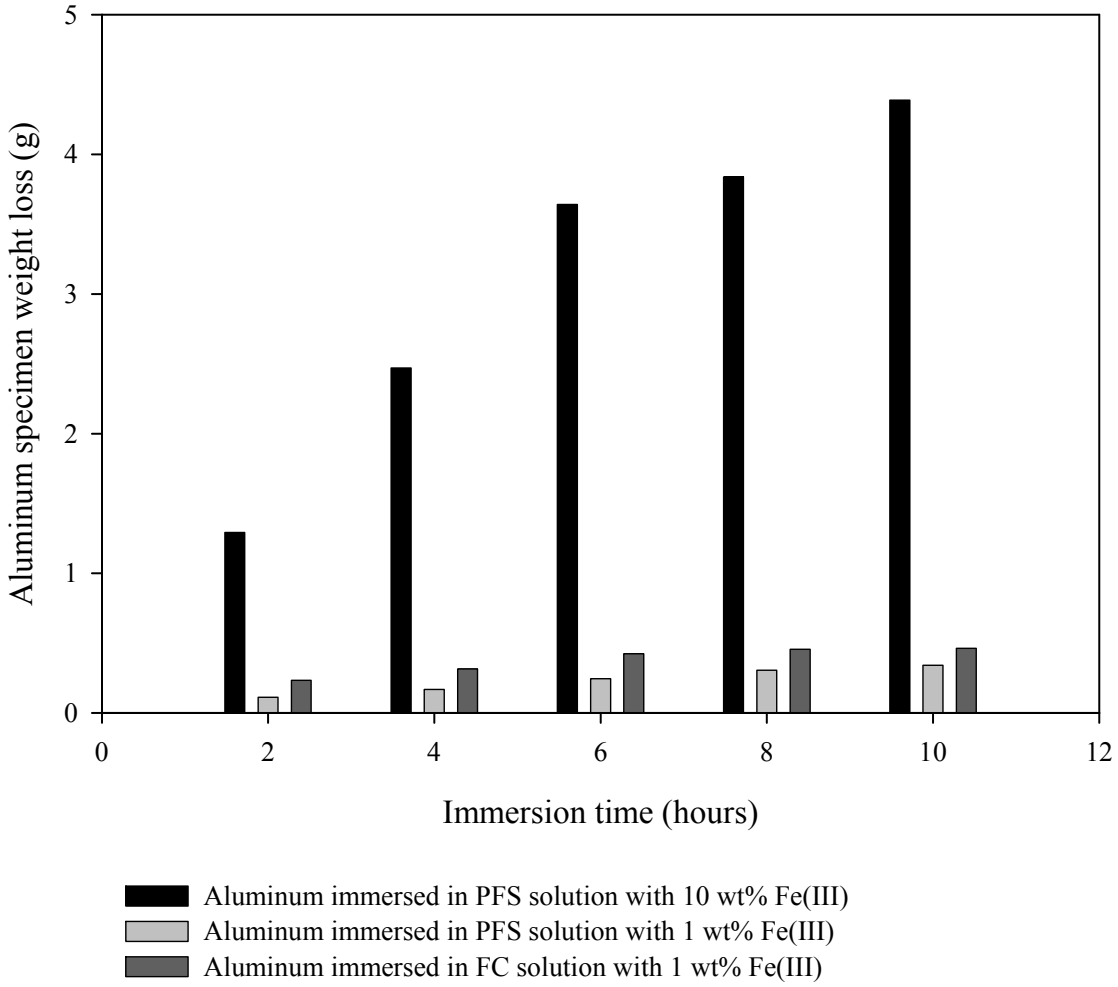


Figure 20. Comparison aluminum corrosion among three different solutions at 35°C

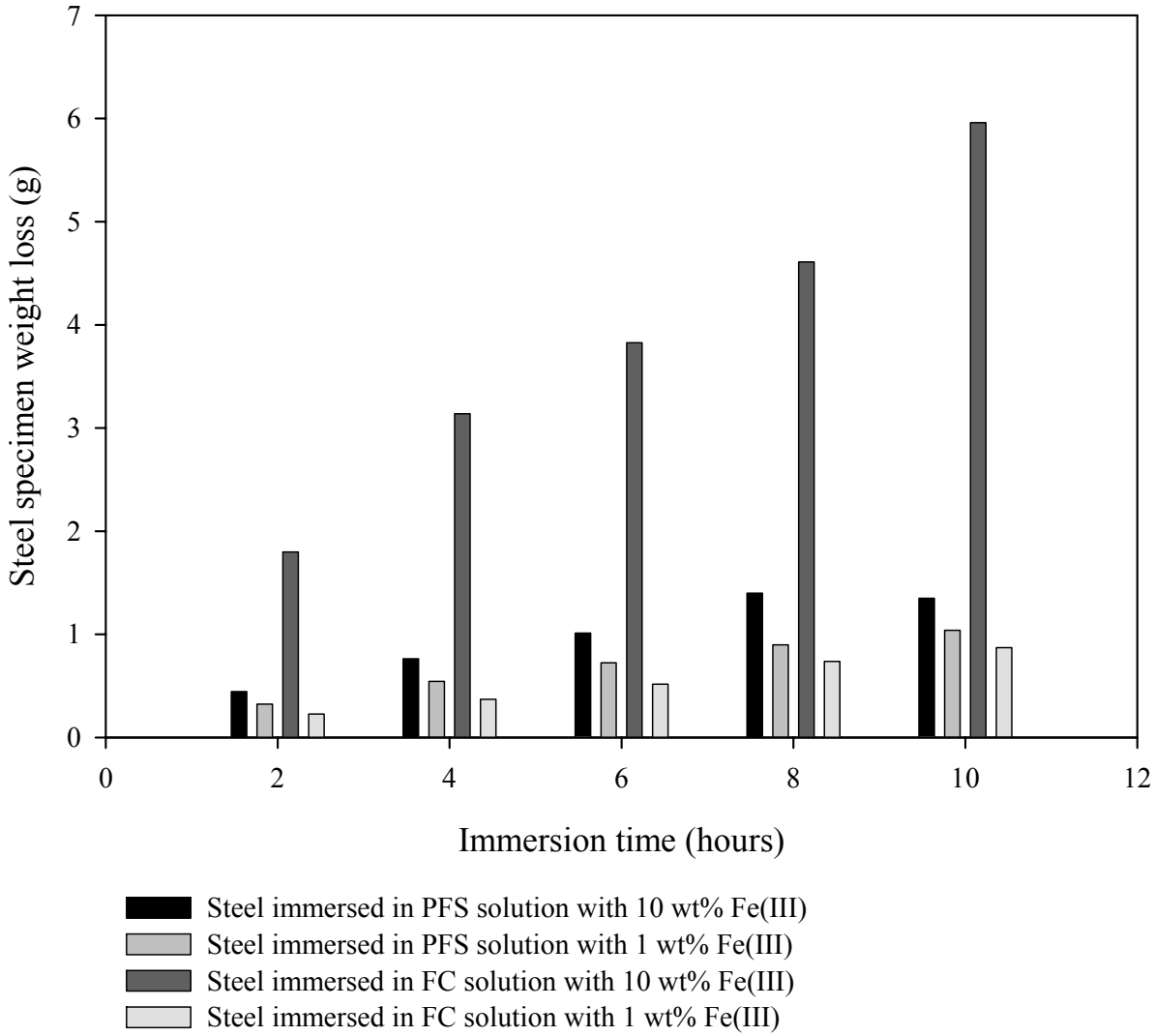


Figure 21. Comparison of steel corrosion among three different solutions at 35°C

Effect of solution and meta

Generally speaking, test results showed that PFS is less corrosive than the FC solution, especially when both contain 10 wt% of Fe(III). For aluminum, all of the weight loss data obtained from the corrosion test justified the trend that PFS will cause less weight loss than an FC solution containing the same concentration of Fe(III). With steel, however, PFS containing 1 wt% Fe(III) caused more weight loss than an FC solution containing 1 wt% Fe(III) at temperatures of 20 °C and 35 °C. When the PFS concentration was 1 wt% Fe(III), its corrosion effect on aluminum was less than steel (Figure 22). With an FC solution containing 1 wt% Fe(III), the weight loss was higher in aluminum in the first several hours. The rate of weight loss of steel, however, surpassed that of aluminum in the latter period of the experiment (Figure 23).

Steel was more resistant than aluminum to both PFS and FC solutions containing 10 wt% Fe(III). Its resistance to the corrosion of PFS solution containing 1 wt% Fe(III), however, was less than aluminum. At the end of the 10-hour experiment, steel also lost more weight than aluminum in the FC solution containing 1 wt% Fe(III). At the immersion time of 10 hours and 20 °C, the weight loss caused by the PFS solution containing 1 wt% Fe(III) was 0.8241 g, or 34% higher than that caused by the FC solution containing 1 wt% Fe(III), which was only 0.6150 g. The weight loss caused by the PFS solution containing 1wt% Fe(III) at 35 °C was 1.0399 g, or 19% higher than that caused by the FC solution containing 1 wt% Fe(III), which was only 0.8714 g.

Both PFS and FC are acid salts, which means solutions containing them will have a low pH value when dissolved in water. An increase in the concentration of acid salts leads to acidification of the solution, and their action or corrosion will be determined to a

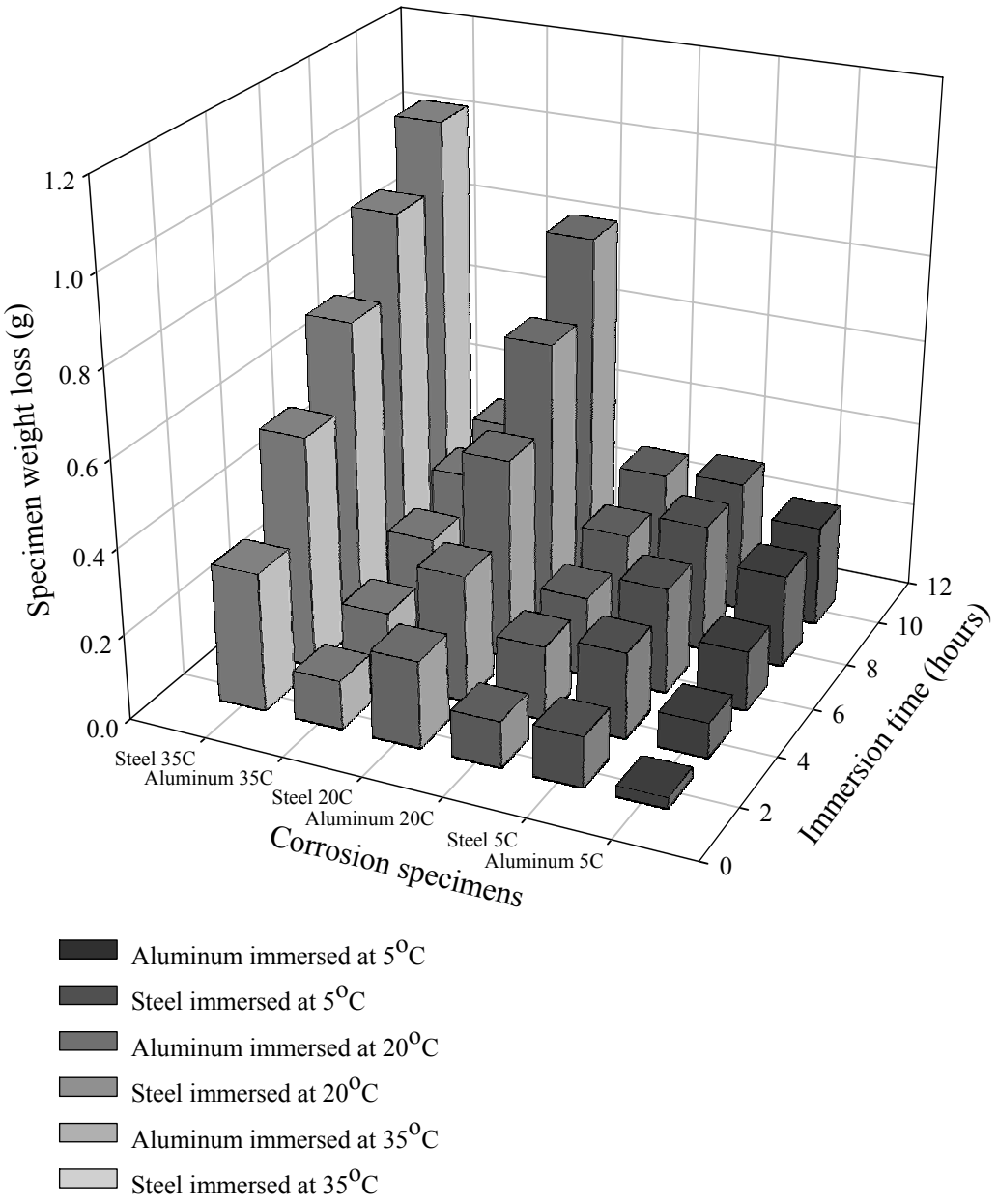


Figure 22. Different corrosion performance between aluminum and steel in PFS solution with 1 wt% Fe(III)

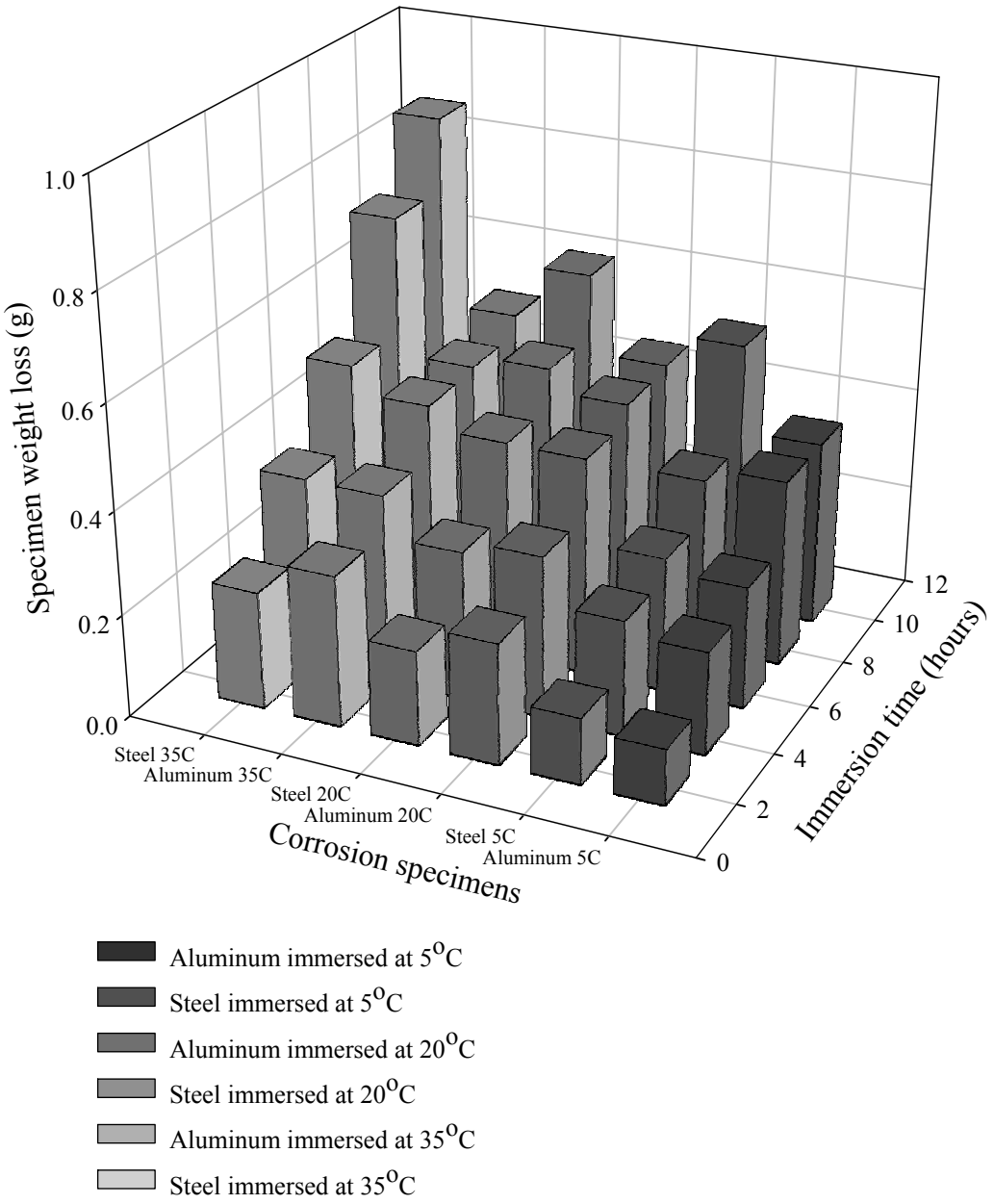


Figure 23. Different corrosion performance between aluminum and steel in FC solution with 1 wt% Fe(III)

large extent by the corrosion behavior change of the given metal with the change in pH of the medium. The electrochemical reaction will produce hydrogen gas, which is shown as (1) and (2). Steel was more resistant to aluminum in acid solution in that the electrochemical potential of iron system lower than aluminum one.

PFS can be expressed with the formula $[Fe_2(OH)_n(SO_4)_{(6-n)/2}]_m$, where m is a function of n (n<2). Since PFS has a higher basicity, it produces H^+ ion when added to water compared to FC, which contains the same amount of iron. Accordingly, the pH value of PFS was higher than that of FC containing the same concentration of Fe(III), which resulted in a lower electrochemical potential and corrosion rate [23], as shown by Equation (24) [21]. Thus, the PFS solution was less corrosive to the facilities than FC when used as a coagulant substitute. This trend was also confirmed by the fact that more hydrogen gas bubbles were produced in PFS solutions compared to those in FC solutions containing the same concentration of Fe(III) when the same metal specimens were used.

$$E = E_0 - \frac{RT}{nF}\ln Q = E_0 - \frac{RT}{nF}\ln\frac{[Fe^{2+}]}{[H^+]^2} \quad (24)$$

The anion in these two coagulants may also contribute to the difference in corrosive behavior. The FC solution contained chloride anion, which is able to attack most metals in an aqueous environment [24]. This anion, when present in a solution, will cause pitting corrosion on the surface of metals. It may act as an anodic accelerator that destroys the protective film on the anodic areas, thereby accelerating the rate of the anodic process. Pits were observed using SEM on all specimens corroded by ferric chloride, no matter aluminum or steel. Moreover, when the specimens immersed in PFS containing SO_4^{2-}, an anion that was not considered an agent as aggressive as Cl^- [25], the surface of the metals were also attacked by pitting, although less severe than the pitting created by Cl^-.

Apparently, chloride anion generated substantial pitting corrosion on the surface of steel. For the SO_4^{2-} anion, it corroded the steel with a different mechanism. The steel specimens were less severely corroded by pitting. Rather, they were more likely to be attacked by intergranular corrosion.

From the SEM results, the pitting number generally increased with the increase of temperature (Figure 24). However, the increase of pit number and diameter with

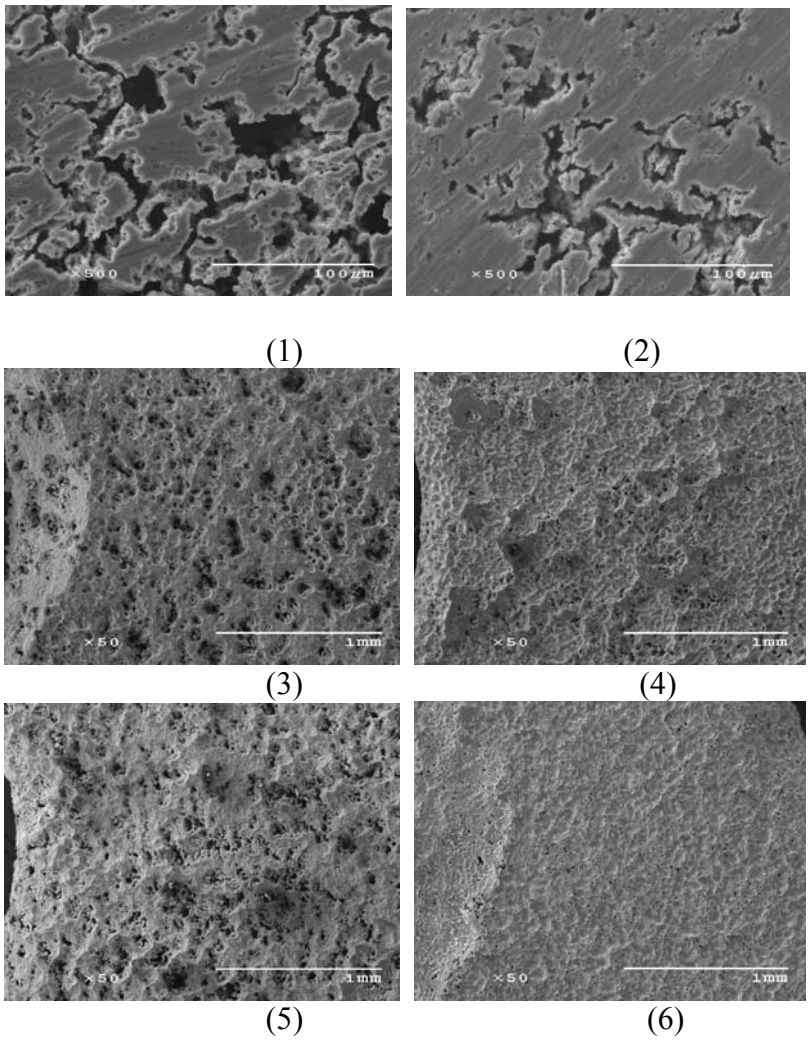


Figure 24. The SEM micrographs of the specimens corroded by different concentrations of PFS and FC for 10 hours at 35°C. (1) Aluminum specimen immersed in FC solution containing 1 wt% Fe(III), (2) Aluminum specimen immersed in PFS solution containing 1 wt% Fe(III), (3) Steel specimen immersed in FC solution containing 1 wt% Fe(III), (4) Steel specimen immersed in PFS solution containing 1 wt% Fe(III), (5) Steel specimen

temperature can not account for the variation of the weight loss caused by temperature change, which may indicate that the pitting corrosion was not the main mechanism that caused the corrosion differences between FC and PFS on both aluminum and steel specimens. The main corrosion behavior, therefore, may contribute to uniform corrosion. Test results showed that the uniform corrosion caused by FC corrosion was much more severe than PFS when both solutions contained 10 wt% Fe(III).

Desulfurization Kinetics

$c_{Cl^-} \sim t$ *Relationships*

The results of the tests on the change of c_{Cl^-} with time under different combinations of initial reactant concentrations are shown in Figures 25, 26 and 27. The trends of the curves in Figures 25, 26 and 27 indicate that none of the reaction orders for $NaClO_3$, $FeSO_4$ and $NaHSO_3$ were zero, since none of those plots is linear. All three of the curves, shown in Figures 25, 26 and 27 rise steeply at the beginning of the reaction and become flat after about 100 seconds, however, each has a different initial rate (within the first 5 seconds). From this, one can determine that the reaction rates of $NaClO_3$, $FeSO_4$ and $NaHSO_3$ are closely correlated with initial reactant concentrations.

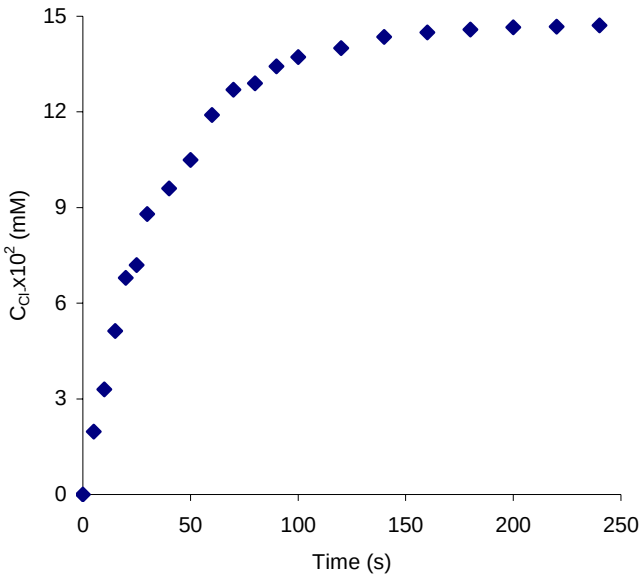


Figure 25. Change of Cl^- concentration with time ($c_{NaClO_3,0}$ = 0.1475 mM, $c_{FeSO_4,0}$ = 29.5 mM and $c_{NaHSO_3,0}$ = 29.5 mM, T = 60 ºC)

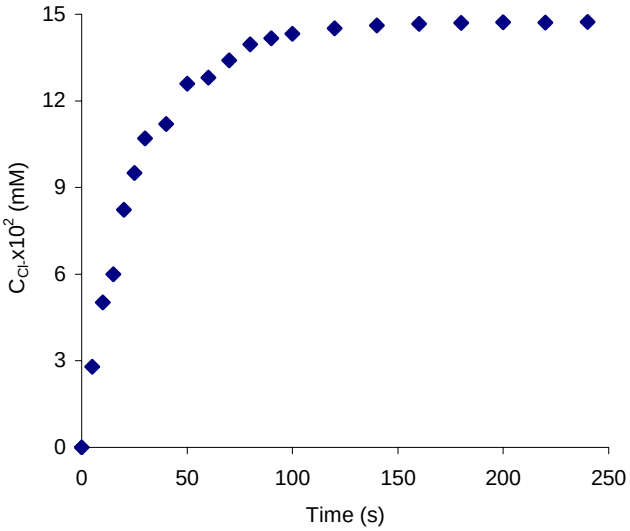


Figure 26. Change of Cl^- concentration with time ($c_{NaClO_3,0}$ = 14.75 mM, $c_{FeSO_4,0}$ = 0.295 mM and $c_{NaHSO_3,0}$ = 29.5 mM, T = 60 ºC)

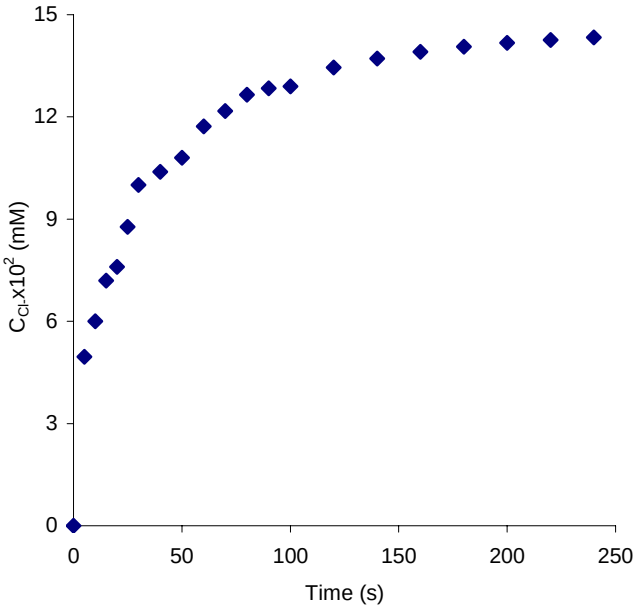


Figure 27. Change of Cl^- concentration with time ($c_{NaClO_3,0}$ = 14.75 mM, $c_{FeSO_4,0}$ = 29.5 mM and $c_{NaHSO_3,0}$ = 0.295 mM, T = 60 ºC)

Derivation of Reaction Orders

The data points in Figures 28, 29 and 30 were derived numerically from Figures 25, 26 and 27 using a tangential method [26]. The resulting linear plots, Figures 28, 29 and 30, each has a regression coefficient higher than 0.95. The slopes of the lines are the reaction orders of reactants $NaClO_3$, $FeSO_4$ and $NaHSO_3$, and are approximately 1.1, 1.1 and 1.4, respectively. Therefore, Equation 7 can be expressed as follows:

$$\frac{dc_{Cl^-}}{dt} = k(c_{NaClO_3,0} - c_{Cl^-})^{1.1}(c_{FeSO_4,0} - 2c_{Cl^-})^{1.1}(c_{NaHSO_3,0} - 2c_{Cl^-})^{1.4} \qquad (25)$$

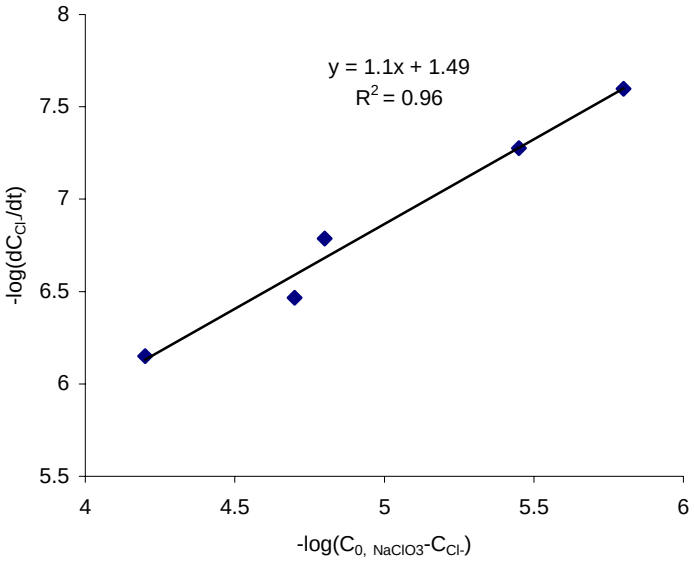


Figure 28. Determination of reaction order of $NaClO_3$ ($c_{NaClO_3,0}$ = 0.1475 mM, $c_{FeSO_4,0}$ = 29.5 mM and $c_{NaHSO_3,0}$ = 29.5 mM, T = 60 ºC)

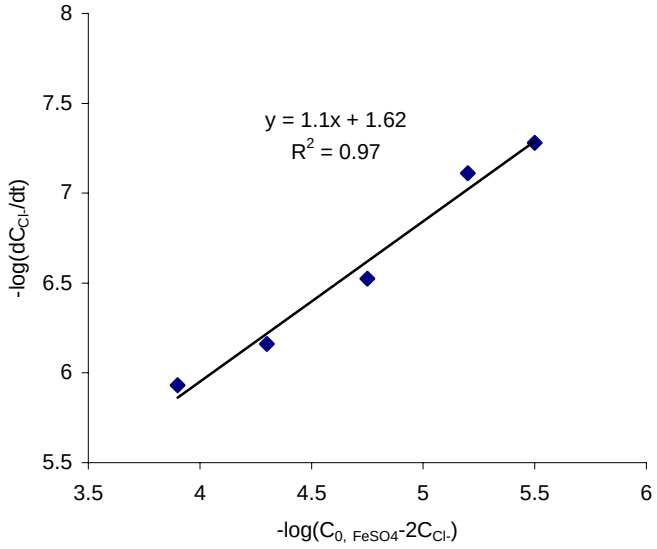


Figure 29. Determination of reaction order of $FeSO_4$ ($c_{NaClO_3,0}$ = 14.75 mM, $c_{FeSO_4,0}$ = 0.295 mM and $c_{NaHSO_3,0}$ = 29.5 mM, T = 60 ºC)

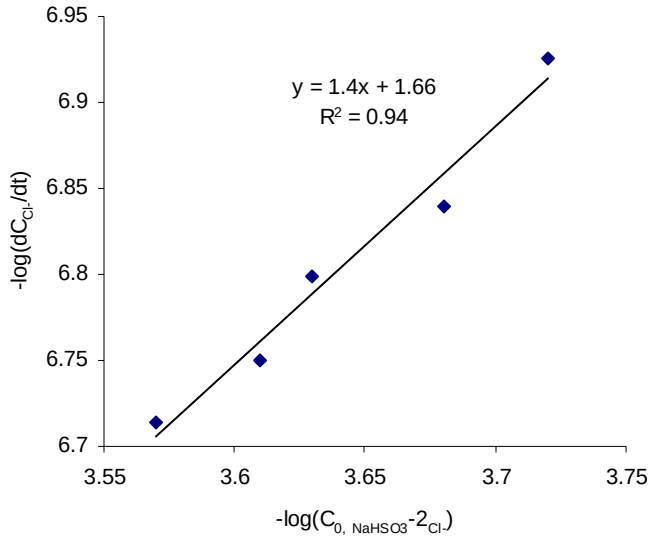


Figure 30. Determination of reaction order of $NaHSO_3$ ($c_{NaClO_3,0}$ = 14.75 mM, $c_{FeSO_4,0}$ = 29.5 mM and $c_{NaHSO_3,0}$ = 0.295 mM, T = 60 ºC)

Establishment of Arrhenius Form

The average concentrations of Cl^- in the reaction system at 150 seconds under temperature 40 ºC, 50 ºC, 60 ºC, 70 ºC and 80 ºC are shown in Table 12. Global rate coefficient *k* at 40 ºC, 50 ºC, 60 ºC, 70 ºC and 80 ºC, calculated with the c_{Cl^-} values in Table 12 and Equation 16, are also listed in Table 11. From these global rate coefficients,

Table 12. Cl^- concentrations (c_{Cl^-}) at 150 s and global rate coefficients calculated for reaction 1 under the different temperature ($c_{NaClO_3,0}$ = 14.75 mM, $c_{FeSO_4,0}$ = 29.5 mM and $c_{NaHSO_3,0}$ = 29.5 mM)

Temperature (ºC)	40	50	60	70	80
c_{Cl^-} (mM)	4.73	7.04	9.02	10.5	11.6
k ($mol^{-2.6}\cdot dm^{2.6}\cdot s^{-1}$)	17.3	43.3	102.3	230.0	494.0

it is evident that rate increases with temperature. The global rate coefficient increases by approximately 100% when temperature increases 10 °C in the temperature range tested, which is consistent with van't Hoff rule [10, 27-8].

Based on the results in Table 11, the relationship between log *k* and 1/T was determined as demonstrated in Figure 31. A regression coefficient of 0.98 in Figure 31 indicates that a good linear relationship between log *k* and 1/T exists. Therefore, the Arrhenius form of reaction 1 can be expressed as

$$k = 7.2\times10^{12}\cdot e^{-\frac{8291}{T}}\,(mol^{-2.6}\cdot dm^{2.6}\cdot s^{-1}) \qquad (26)$$

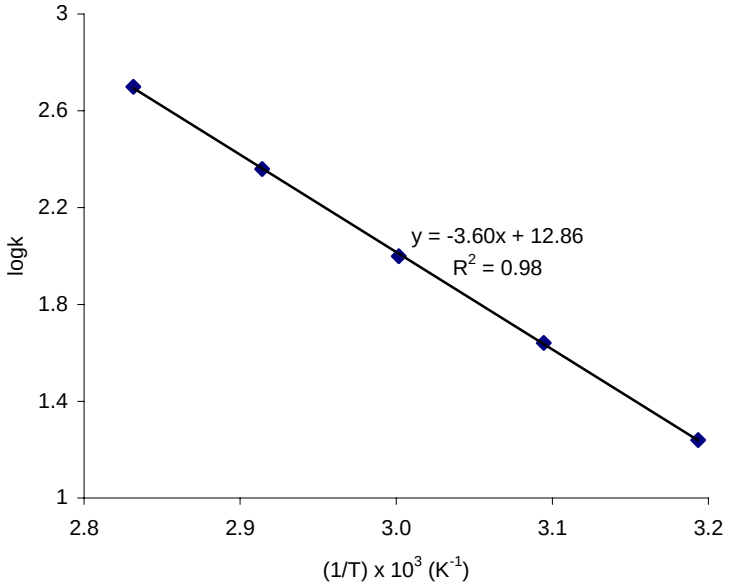


Figure 31. Determinations of activation energy and the pre-exponential factor in Arrhenius form ($c_{NaClO_3,0}$ = 14.75 mM, $c_{FeSO_4,0}$ = 29.5 mM, $c_{NaHSO_3,0}$ = 29.5 mM and t = 150 s)

In conclusion, the reaction between $NaClO_3$, $FeSO_4$ and $NaHSO_3$, potentially used for sulfur removal from flue gas, was characterized. A kinetic model, including reaction orders and activation energy, has been established by tracking the change of the

concentration of the chlorine ion with time during the reactions with different initial reactant concentrations. This study is essential in understanding the underlying chemical mechanism of the new sulfur removal technique, which can provide the basis for the design and optimization of the process.

CONCLUSIONS

Absorption of sulfur dioxide from a mixed gas stream was investigated by sparging it into a stirred benchtop reactor containing a solution of ferrous sulfate with sodium chlorate added as an oxidant. The sole reaction product was polymeric ferric sulfate (PFS), a highly effective coagulant useful in treatment of drinking water and wastewater. The reaction took place near atmospheric pressure and at temperatures of 30-80°C. SO_2 removal efficiencies greater than 90% were achieved, with ferrous iron concentrations in the product less than 0.1%.

A factorial analysis of the effect of temperature, oxidant dosage, SO_2 concentration, and gas flowrate on SO_2 removal efficiency was carried out, and statistical analyses were performed. The results suggest that SO_2 removal efficiency is improved by increasing dosages of oxidant, while it is reduced by an increase in temperature. It is postulated from reaction stoichiometry that the iron reaction is more competitive for the available oxidant at the higher temperatures, which reduced desulfurization efficiency.

PFS quality was evaluated by wet chemistry methods to verify that the process was capable of consistently producing high quality PFS. Quality parameters examined were total iron concentration, ferrous iron concentration, basicity, density, and pH. It was found that the basicity of PFS could be adjusted by varying how long the desulfurization reaction was continued after all Fe(II) was converted to Fe(III). In addition, dried, powdered samples of PFS were analyzed by x-ray diffraction to determine whether drying temperature had an effect on relative crystallinities. All samples examined were highly amorphous.

The PFS product was used in pilot-scale tests at a municipal water treatment facility and gave good results in removal of turbidity and superior results in removal of disinfection byproduct precursors (TOC, DOC, UV-254) when compared with equal doses of ferric chloride. PFS is also better than other coagulants such as aluminum sulfate in other performance of water treatment. For example, it is better than aluminum sulfate in the removal of As.

In addition, tests have shown that PFS is a less corrosive material than ferric chloride. Therefore, application of FFS in water treatment plants will help to improve the working environment of water treatment plants and to protect pipelines of water treatment plants.

REFERENCES

1. Chinese Administration of Chemical Engineering (CACE), (1992) "Chinese Polymeric Ferric Sulfate Quality Standard." HG 2153-91, Beijing, China.
2. Y. Mikami, M. Yanayi, H. Molita and T. Tonaiyama, PPM 5. (1984) 24-32 (in Japanese).
3. K. A. Gary, (1988) *The Preparation, Characterization, and Use of Inorganic Iron (III) Polymers for Coagulation in Water Treatment*, The John Hopkins University, Ph.D. Thesis, pp. 123.
4. W. Schneider and B. Schwyn, (1987) The hydrolysis of iron in synthetic, biologic and aquatic media. In: *Aquatic Surface Chemistry* (Stumm, W. Ed.). John Wiley & Sons. New York, 167-196.
5. Y. Shen, (1992) Ph.D. Dissertation, Synthesis and characterization of polyaluminum coagulants for water treatment. Pennsylvania State University.
6. R. C. Cheng, S. Liang, H. H. Wang and M. D. Beuhler, (1994) Enhanced coagulation for arsenic removal, *J. Am. Water Works Association.* 86 (9), 79-90.
7. N. Berkowitz, (1979) *An Introduction to Coal Technology*, Academic Press, New York.
8. J. Mathews, K. Fink, (1999) *Numerical Methods with MATLAB* , 3rd ed.; Prentice-Hall, Upper Saddle River, NJ.
9. G. Parravano, J. J. Martin, D. L. Katz, (2000) *Elements of Chemical Reaction Engineering*, 3rd ed.; Prentice Hall PTR, New Jersey.

10. M. Fan, (1997) *Research on New Desulfurization Technologies*, Ph.D. Thesis, Research Center for Eco-Environmental Sciences of the Chinese Academy of Sciences.

11. **M. Fan, R. C. Brown**, S. Sung and Y. Zhuang, (2002) A process for synthesizing polymeric ferric sulfate using sulfur dioxide from coal combustion, *International Journal of Environment and Pollution,* 17(1), 102-109.

12. J. Dousma and P. L. Bruyn, (1976) Hydrolysis-precipitation studies of iron solutions. l. model for hydrolysis and precipitation from Fe(III) Nitrate solutions, *J. Colloid and Interface Sci*., 59(3), 527-539.

13. L. S. McNeill and M. Edwards, (1973) Predicting As removal during metal hydroxide precipitation, *J. Am. Water Works Association,* 89 (1), 75-85.

14. M. L. Pierce and C. B. Moore, (1982) Adsorption of arsenic and arsenate on amorphous iron hydroxide. *Water Research.* 16 (7), 1247-1253.

15. M. Fan and Y. Zhuang, (1998) Research on a new desulfurization process with $FeSO_4$ solution as an absorbent. *Environ. Sci.* 19 (1), 5-8.

16. R. J. Knight and R. N. Sylva, (1974) Precipitation in hydrolyzed iron (III) solutions. *J. Inorganic Nuclear Chemistry.* 36 (2), 591-597.

17. H. Tang and W. Stumm, (1987) The coagulation behaviors of Fe (III) polymeric species-I. Preformed polymers by base addition. *Water Research.* 21 (1), 115-121.

18. J.G. Hering, P. Y. Chen, J. A. Wilkie, M. Elimelech, and S. Linag, (1996) Arsenic removal by ferric chloride. *J. Am. Water Works Association.* 88 (4), 155-167.

19. W.J. Viessman and M. J. Hammer, (1998) Chemical treatment processes. *Water Supply and Pollution Control*, 6th edition. Addison Wesley Longman. Menlo Park, CA.

20. S. W. Hathaway and F. Jr. Rubel, (1987) Removing arsenic from drinking water *J. Am. Water Works Association.* 79 (8), 61-65.

21. N. D. Tomashov, (1966) Theory of corrosion and protection of metals: The science of corrosion, Macmillan, New York, 1966, pp. 143-144.

22. V. L. Snoeyink and D. Jenkins, (1980) Water Chemistry, Wiley, New York, pp. 66-67.

23. J.M. Zhao and Y. Zuo, The effects of molybdate and dichromate anions on pit propagation of mild steel in bicarbanate solution containing Cl^-, (2002) *Corros. Sci.*, 44 (9), 2119-2130.

24. U. Evans, (1979) *An Introduction to Metallic Corrosion*, Edward Arnold, London, U.K.

25. E.A. Abd El Meguid, N.A. Mahmoud and S.S. Abd El Rehim, (2000) The effect of some sulfur compounds on the pitting corrosion of type 304 stainless steel, *Mater. Chem. Phys.*, 63(1), 67-74.

26. J. Mathews and K. Fink, (1999) *Numerical Methods with MATLAB* , 3rd ed.; Prentice-Hall, Upper Saddle River, NJ, 1999.

27. G. Parravano, J. J. Martin and D. L. Katz, (2000) *Elements of Chemical Reaction Engineering*, 3rd ed.; Prentice Hall PTR, New Jersey.

28. O. Levenspiel, (1996) *The Chemical Reactor Omnibook*, Oregon State University Book Stores, Corvallis.

APPENDICES

A List of Publications Supported by This DOE Award (DE-FG26-00NT40812)

1. Butler, D. A., M. Fan, R. C. Brown**,** J. V. Leeuwen, S. Sung and B. Duff, (2005). Pilot scale water treatment study of polymeric ferric sulfate synthesized using SO_2, *Chemical Engineering* , 44(3), 413-419.
2. Butler, A. D., M. Fan, R. C. Brown, A. T. Cooper, J. V. Leeuwen and S. Sung**,** (2004). Absorption of Dilute SO_2 Gas Stream with Conversion to Polymeric Ferric Sulfate for Use in Water Treatment, *Chemical Engineering Journal*, 98, 265-273.
3. Shi, Y., M. Fan, R. C. Brown, Shihwu Sung and J. V. Leeuwen, (2004). Comparison of corrosivity of polymeric sulfate ferric and ferric chloride as coagulants in water treatment, *Chemical Engineering and Processing,* 43(8), 950-959.
4. Lloyd, H., A.T., Cooper, M. Fan, R. C. Brown and J. V. Leeuwen. Comparison of different coagulants in the treatment of tidal Savannah River water, *Journal of Environmental Engineering*, (submitted).
5. Fan, M., R. C. Brown, S. Sung, C. P. Huang, S. K. Ong and J. V. Leeuwen, (2003). Comparison of polymeric and conventional coagulants in arsenic (V) removal, *Water Environment Research,* 75(4), 308-313.
6. Fan, M., R. C. Brown, Y. Zhuang, A. T. Cooper and M. Nomura, (2003). Reaction kinetics for a novel flue gas cleaning technology, *Environmental Science & Technology,* 37(7), 1404-1407.
7. Fan, M., R. C. Brown and S. Sung, (2003). Photoacoustic measurement of iron in composite coagulant, *Chemical Engineering and Process,* 42(7), 553-559.
8. Fan, M., S. Sung, R. C. Brown, T. D. Wheelock and F. C. Laabs, (2002). Synthesis, characterization and coagulation performance of polymeric ferric sulfate, *Journal of Environmental Engineering*, 128(6), 483-490.
9. Fan, M., R. C. Brown, S. Sung and Y. Zhuang, (2002). A process for synthesizing polymeric ferric sulfate using sulfur dioxide from coal combustion, *International Journal of Environment and Pollution,* 17(1), 102-109.
10. Hendrich, S., M. Fan, S. Sung, R. C. Brown, M. L. Mazur, R. Myers and G. S. Osweiler, (2001). Toxic evaluation of polymeric ferric sulfate, *International Journal of Environmental Technology and Management*, 1(4), 464-471.